THE WEST ANTARCTIC ICE SHEET: BEHAVIOR AND ENVIRONMENT
ANTARCTIC RESEARCH SERIES, VOLUME 77, PAGES 257-281

ICE STREAMS B AND C

I. M. Whillans
Byrd Polar Research Center and Department of Geological Sciences, Ohio State University, Columbus, Ohio

C. R. Bentley
Geophysical and Polar Research Center, University of Wisconsin, Madison, Wisconsin

C. J. van der Veen
Byrd Polar Research Center and Department of Geography, Ohio State University, Columbus, Ohio

The mapping and description of the kinematics and dynamics of ice streams B and C are reviewed. The discussion centers around the themes of why ice streams are fast despite small driving stress and why and how ice streams change with time. The mapping has described the limits to the ice streams, their surface and bed features and crevasses. For ice stream B, velocities are in excess of those needed to evacuate current snow accumulation, so the catchment of ice stream B is thinning. Also, ice stream B is widening and slowing. In contrast, the lower and middle reaches of ice stream C have mainly stopped and are thickening. The upper portion of ice stream C is active, and there must be some special ongoing activity at the region joining active and stopped ice. The bed under ice stream B has a layer of soft sediment. This sediment has probably been in traction from the ice above and the process is likely active now. Debris has collected in a delta-like feature under the mouth of ice stream B. An analysis of the budget of forces shows that gravitational action on ice stream B is opposed mainly from the sides, meaning that the bed is nearly perfectly lubricated. A calculation along the flowline shows where the ice stream begins and how some of the characteristics change along-glacier. For ice stream C the reaction to the driving stress is from the bed. Various suggested hypotheses for the controls on ice stream behavior are reviewed in the light of measurement programs that were targeted to test them. The analysis does not favor dominance of the hypotheses of basal heat feedback, global warming, piracy, height above buoyancy, deforming bed, ongoing surge, or active volcanism in ice stream behavior. Rather an active ice stream has a very weak bed, probably because it is soft and moldable, and frictional drag comes from the sides. The cause of switches in time of basal drag are not yet known.

INTRODUCTION

Ice stream B (Figure 1) is the archetypal example of an ice stream. An ice stream contrasts with other outlet glaciers in that these other glaciers are fast but have very steep surface slopes, meaning that the gravitational driving stress is large. An example of such an outlet glacier is Byrd Glacier, which passes through the Transantarctic Mountains. It achieves velocities of 0.8 km a^{-1} under a mean driving stress of 220 kPa (calculated from elevation decrease from 550 m to 150 m over 40 km and ice thickness 2500 m [*Whillans et al.*, 1989]), yet as discussed next, ice stream B achieves similar speeds under a driving stress of 15 kPa, only 7% of that of Byrd Glacier. The other distinguishing feature of ice streams is the lack of close bed-topographic control on the routes. These characteristics lead to the ice streams catching special scientific attention .

This first anomaly of the flow of ice stream B is displayed in Figure 2. Driving stress is only about 15 kPa (3rd panel), yet speeds reach 800 m a^{-1} (4th panel). Moreover, over the span from –200 km to +50 km speed becomes larger as the gravitational forcing becomes smaller. Such a relation is counter to the concepts of classical glaciology. This mysterious inverse relation between forcing and response calls for an explanation.

Next to ice stream B is ice stream C (Figure 3). Its presence is evident on imagery, but its middle and lower reaches have small speeds (Figure 3; [*Whillans and Van*

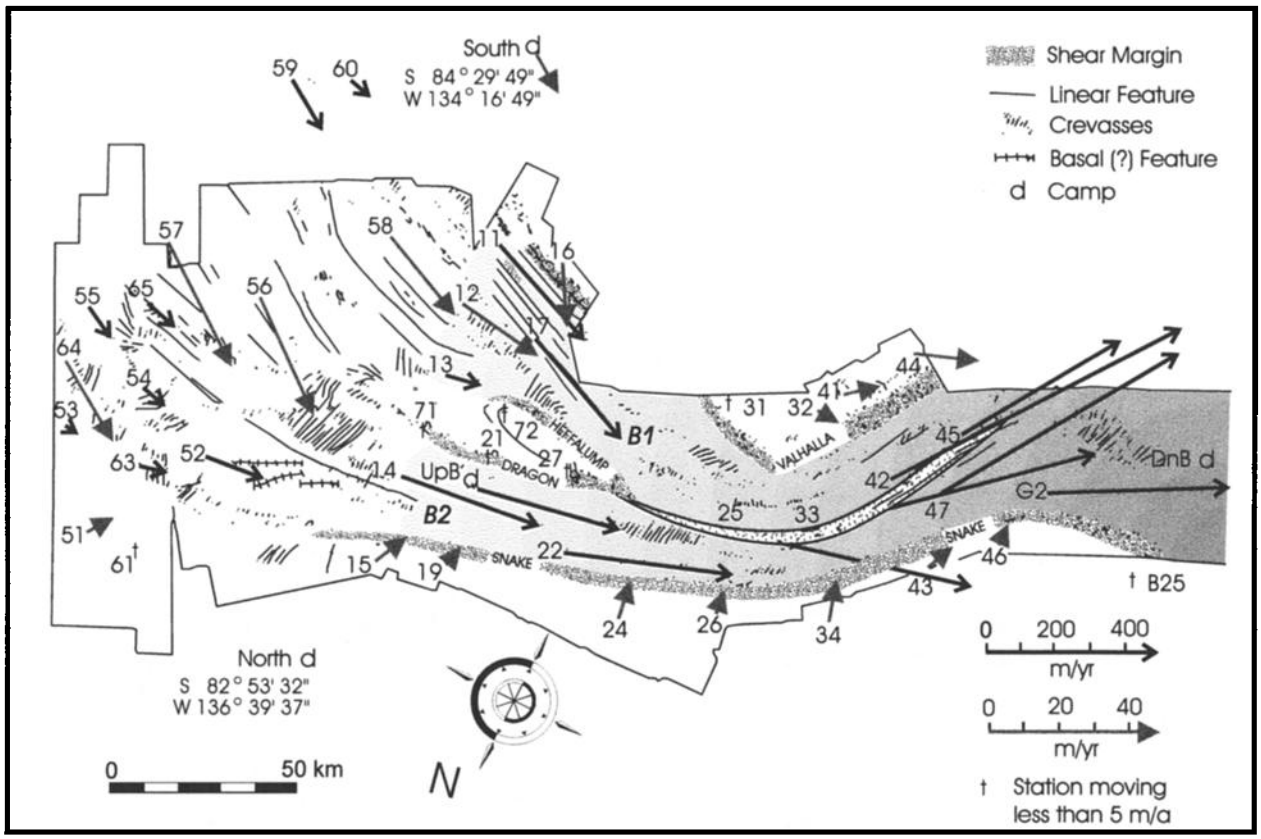

Fig. 1. Ice stream B showing surface features and velocities. The features derive from interpretations of aerial photos and satellite images, the velocities from ground-based surveys [*Whillans and Van der Veen,* 1997]. Reproduced from the Journal of Glaciology with permission from the International Glaciological Society and the authors.

der Veen, 1993]) and buried crevasses indicating former activity [*Bentley et al.,* 1985]). The characteristics of ice stream C and the history of its discovery are discussed in the companion paper by *Anandakrishnan et al.* (this volume) and raise a second mystery: how and why the ice streams change.

In this report some of the evidence relating to these two mysteries (fast flow under small driving stress for ice stream B and to stoppage of ice stream C) is reviewed and the current status of the problems of ice stream flow is summarized.

MAPPING THE ICE STREAMS

A combination of aerial photography, satellite imagery, and radio-echo sounding has been used to map the ice streams. A compilation of much of the data is presented in Figures 1 and 3. The first mapping of the surface and bed elevations and ice thickness was carried out as part of the NSF-SPRI-TUD radio-sounding program of the 1960's and 1970's [*Robin et al.,* 1970; *Rose,* 1979]. Newer, more detailed maps stem principally from extensive airborne radar sounding carried out in 1984-85 [*Shabtaie and Bentley,* 1987, 1988; *Shabtaie et al.,* 1987] and 1988-89 [*Retzlaff et al.,* 1993] with ground control by satellite tracking [*Whillans and Van der Veen,* 1993]. The 1984-85 set of flights were reconnaissance in nature and employed analog recording of the data, whereas the 1988-89 flights were on regularly spaced grids with 5- or 10-km line spacings and data were recorded digitally.

Part of a satellite image is shown in Figure 4*a*. It reveals crevasses, drift mounds, flow traces and ridges and troughs. A chaotic zone of crevasses and outboard arcuate crevasses marks each lateral boundary (Figure 4*b*; also discussed in *Raymond et al.* [this volume]). The interstream ridges (except ridge A/B) have very simple smooth surfaces that slope toward the ice streams. The along-flow beginning and end to ice stream flow are not clearly evident in the images or photos.

The surface of ice stream B exhibits an irregular topography of uncertain origin. Some small features are migrating with time. Most features are too small to depict in Figures 1 and 3. An image trackable feature 'a', near the mouth of ice stream B, is traveling down-

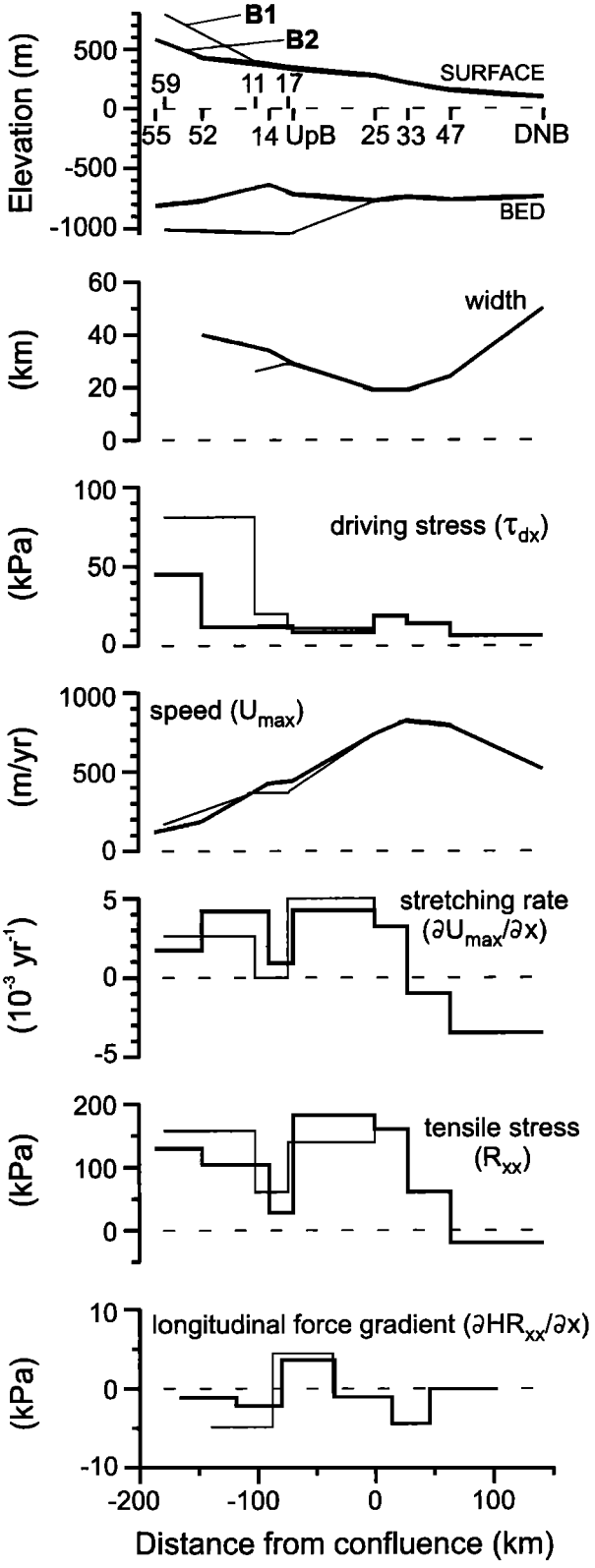

Fig. 2. Data and steps in computation of budget of forces. Origin of coordinate system is at station 25 (near the junction of tributaries B1 and B2). Elevations and station names (top panel) and speeds (U_{max}, 4th panel) from *Whillans and Van der Veen* [1993]. Bed elevation (top panel) from *Retzlaff et al.* [1993]. Width of ice stream, W, from distance between zones of severe crevasses as evident on photographs and satellite images (at the upper end of the ice stream this width differs from that of *Shabtaie et al.* [1987], who based it on correlation of zones of intense clutter between ice-sounding radar flight lines). Driving stress (3rd panel), stretching rate, longitudinal tensile stress, and longitudinal force gradient are computed from data in the panels above. Resistive stresses involve the rate factor, B = 540 kPa $a^{1/3}$, corresponding to the depth-weighted mean using the temperature profile measured at the UpB camp [*Engelhardt et al.*, 1990] and the temperature dependence given in *Hooke* [1981].

glacier [*Bindschadler and Vornberger*, 1998]. Near the head of ice stream B, at UpB, many topographic features are migrating up-glacier [*Hulbe and Whillans*, 1997]. In contrast, the boundary between ice streams B1 and B2, downstream of the Unicorn and containing stations 25, 33, 42, and 45 (Figure 1), persists as a suture zone for 250 km down-glacier from their merger.

Most shear margins to the ice streams B and C are not distinct in surface topography. Exceptions to this remark are a few margins that contain surface valleys, such as the down-glacial portion of the northern shear margin (the Snake) of ice stream B [*Shabtaie et al.*, 1987] and the northern margin of ice stream A. Northern ice streams D and E are different from ice streams B and C, being bounded by especially steep slopes over a zone about 1 km wide just outboard of the shear margins [*Stephenson and Bindschadler*, 1990]. For ice streams B and C, the lack of major relief in most of the margins demonstrates that surface relief is not a necessary characteristic.

Also, there is no clear association of ice-stream location with subglacial topography. Much of ice stream B1 overlies a deep subglacial trough, but part also overlies a subglacial ridge. The upper parts of ice stream B1 are associated with a deep-lying bed, but so are the neighboring inter-stream ridges. There is a shallower trough beneath ice stream B2 near station UpB, but it trends diagonally across the ice stream, not along its axis. From a contour map of subglacial topography alone, it would be very difficult to predict where ice streams might form. There is some indication that the association between subglacial troughs and ice-stream axes may become closer up-glacier where the subglacial relief is greater [*Shabtaie and Bentley*, 1988], but it is not possible to test this hypothesis definitively because the positions of some of the ice-stream boundaries are not well known in that region.

Close to the Ross Ice Shelf, the combined trunk of ice stream B widens into a nearly flat area known as an "ice plain." There the mean surface slope is only 3.5×10^{-4} and surface elevations are only a few tens of meters above hydrostatic equilibrium in the ocean [*Shabtaie and Bentley*, 1987].

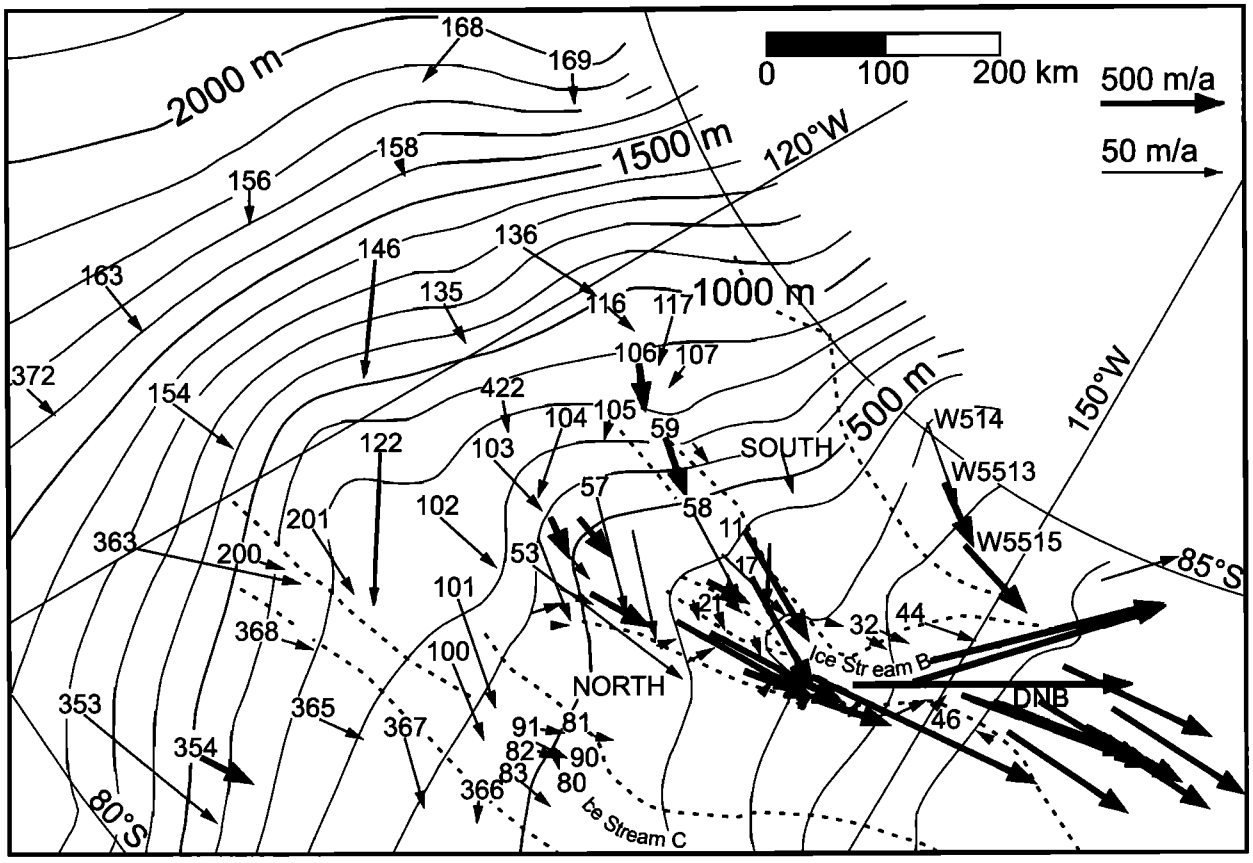

Fig. 3. Ice streams B and C and their catchment areas with velocity determinations superposed. Velocities are *from Price and Whillans* [1998]. Shear margins are from *Shabtaie et al.* [1987].

The surfaces of ice streams are lower than those of the interstream ridges to either side. For ice stream B the slope from interstream ridge into ice stream drives ice flow across the shear margin into the ice stream from the sides. Speeds on the interstream ridges are about that expected to balance the measured surface accumulation rate [*Whillans and Van der Veen,* 1993].

At the head of the small-activity ice stream C there is a bulge in the surface [*Joughin et al,* 1999; *Spikes et al,* 2000]. This form is believed to be linked to the future reactivation of ice stream C but the precise location of the future active ice stream is not clear.

In short, the locations of the ice streams are not definitively associated with basal topography. Their locations must be at least partially controlled by basal or internal conditions, particularly in their more downglacier portions. Inland, the lateral boundary between inland-ice flow and ice-stream flow is not clearly understood.

Exposed Crevasses

Broad-scale maps of location and type of exposed crevasses have been made using photos and satellite imagery. The first maps are based on aerial photography [*Vornberger and Whillans,* 1990]. Later maps include information from SPOT imagery (Figure 1). Other imagery that can be useful are DISP [*Bindschadler and Vornberger,* 1998] and AVHRR [*Bindschadler and Vornberger,* 1990]. LANDSAT is not helpful because ice stream B lies well beyond its latitudinal range. Figure 1 includes simplified tracings of crevasse patterns on ice stream B.

A characteristic feature of ice streams is the crevassed shear margins. These margins separate the active ice streams from the slowly moving interstream ridges. The pattern of crevasses within a shear margin is shared with other glaciers with large strain rates at the sides, but the pattern is on a very grand scale in the case of ice streams. An image of the Dragon is shown in Figure 4*b*. *Raymond et al.* [this issue] discuss shear margins more thoroughly. As observable with visible imagery, a shear margin begins with a series of irregular crevasses or buckles in ice flow. The Dragon begins with a fan shaped set of crevasses (Figure 4*a*). Within a well-developed shear margin the crevasses are arcuate on the outboard side and, with drift mounds, form a chaotic zone on the inboard side of the shear margin

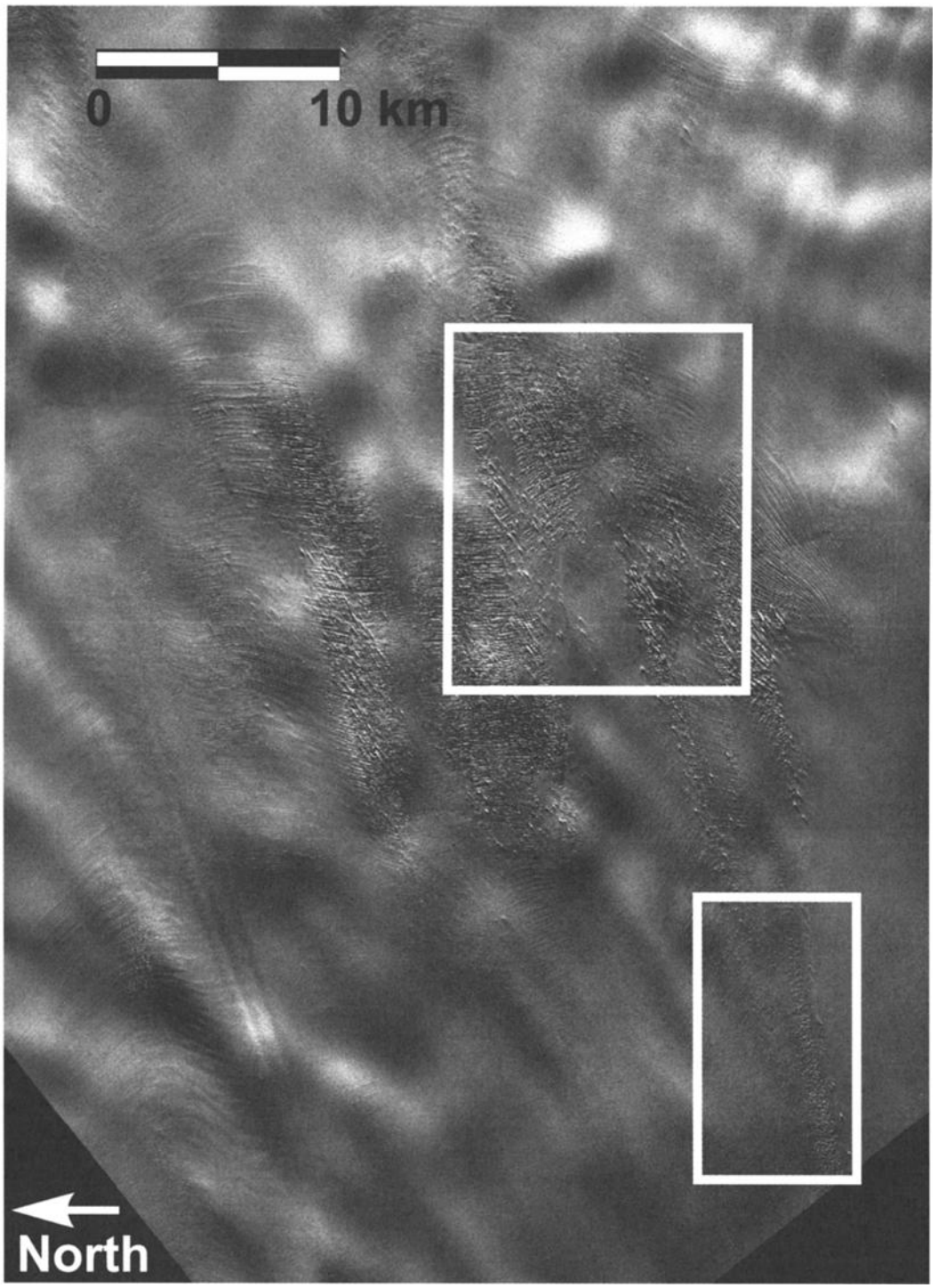

Fig. 4a. Head of ice stream B, between stations 56 and 14 on Figure 1. Flow traces cross the entire image from top to bottom. Most crevasses are transverse to ice motion (which is top to bottom). Drift mounds are aligned diagonally upper-left to lower-right. [SPOT High Resolution Visible image, K092 J569, December 15, 1989, 15:29 GMT; solar azimuth: 83.1°; solar elevation: 24.1°].

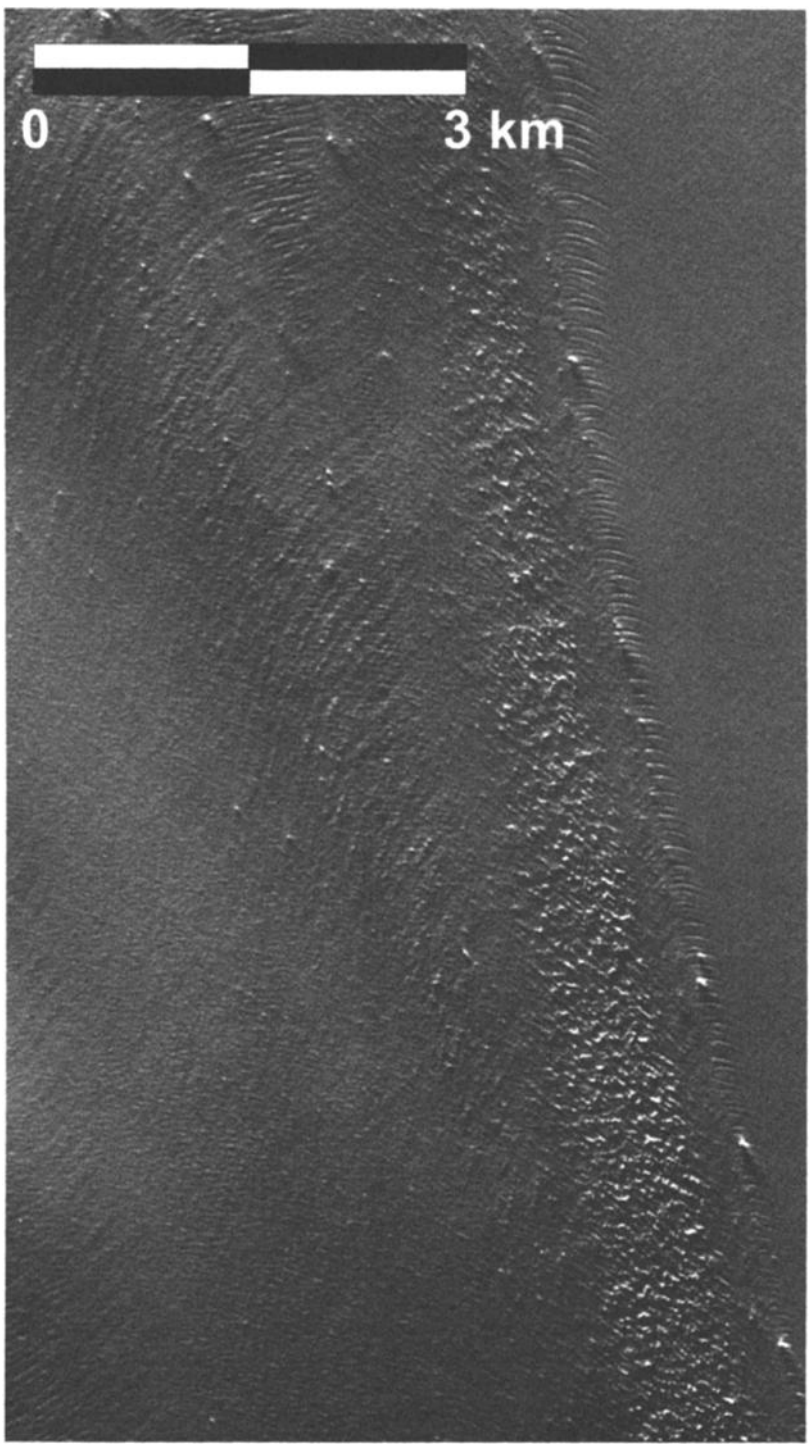

Fig. 4*b*. Subscene from Figure 4*a* showing the Dragon shear margin. The active ice stream moves from top to bottom of the image on the left-hand side. The uncrevassed region to the right is the nearly stagnant interstream ridge (Unicorn). The rightmost crevasses are arcuate and hooked down-glacier.

(Figure 4*b*). Ice from the interstream ridge flows laterally into the shear margin where it is taken up as part of ice stream flow. The shear margins can retain their simple forms over distances in excess of 250 km (in the case of the Snake).

Most observable crevasses in the body of the ice stream are transverse crevasses (for example in Figure 4*a*). Measurements of velocity, reported on below, show that the flow pattern in the ice stream is, to a first approximation, simple lateral shear. Crevasses formed under such a regime are diagonal to flow, but with age and down-glacial transport existing crevasses continue to open and rotate. In such a simple shear regime these crevasses are widest when they are transverse to flow. It is these that are most readily observed. During rotation the crevasses experience strike-slip shearing along their lengths. This leads to complex shapes and folding of intercrevasse slivers. Further rotation causes the crevasses to close.

There is a much smaller crevasse density near the kinematic centerline of the ice stream (left-hand portion of Figure 4*a*). This is a site of small lateral shear stress, meaning that there is less along-crevasse shearing. Existing crevasse bridges are less distorted and less evident in visual inspections near the centerline. The small crevasse density and the less distortion of bridges at the centerline mean that there are many sites where the Twin Otter aircraft can make safe landings. This is the reason that most point determinations of ice-stream velocity are near the kinematic centerline (cf. Figure 1).

Most of the crevasses in the ice stream are bridged and most bridges sag. Some bridge sections fall, leaving a hole. Such cavities disrupt the surface wind pattern. Snow drift collects downwind of the cavity to form drift mounds [*Vornberger and Whillans,* 1990]. Often the hole is rebridged but the drift mound remains visible. The drift mounds in Figures 4*a* and 4*b* and seen in photos and overflight are believed to form in this way. It is sagging bridges and drift mounds that can be mapped and tracked with time to determine motion [*Scambos and Bindschadler,* 1993; *Bindschadler et al.,* 1996; *Whillans and Tseng,* 1995; *Whillans et al.,* 1993; *Whillans and Van der Veen,* 1997].

Crevasses Intersect at Oblique Angles

The simple viewpoint is that considering that the void within a crevasse cannot support tensile stress perpendicular to crevasse orientation, a new crevasse formed in ice with existing crevasses should be parallel or perpendicular to earlier crevasses [*Van der Veen,* 1998]. Some glaciers exhibit this pattern (e.g. Mulock Glacier in the Transantarctic Mountains [*Swithinbank,* 1988, page B31], also Skeiðarárjökull, Iceland, during a surge [*Björnsson,* 1998, cover photo], arctic glaciers [*Herzfeld,* 1998, figures 168 and 190]). On the ice streams, the observation of frequent oblique crevasse intersections (Figure 4*c*) indicates that new crevasses must form in unfractured ice, beneath the depth of penetration of preexisting crevasses. Old crevasses must heal at depth because otherwise the older crevasse would open wider instead of a new crevasse forming. A speculation on why pre-existing crevasses are not foci for new crevasses is that the deep extensions of crevasses are not fractures but are recrystallization fronts that heal and strengthen with strain [*Whillans et al.,* 1993]. Other models for such behavior are possible. For an arctic glacier in Canada, *Hambrey and Müller* [1978, p. 59] make similar observations but suggest upward water migration as the physical process, a process not feasible on the ice streams. The common interpretation is that deep parts of crevasses can heal and new crevasses form at other angles.

The speed of upward growth of new crevasses in ice streams is not known, it could be nearly instantaneous or very slow, perhaps with crevasses not always reaching the surface. The lack of resolution of this issue means that crevasse age estimates based on crevasse depth requires some line of argument about past depth of the upper portion of crevasses.

There are some special patterns to crevasses observed on ice stream B. Splaying crevasses just upglacier of the DnB camp (Figure 1) indicate lateral spreading and crevasse advection as the ice stream fans out toward the ice shelf. The Dragon shear margin (Figure 4*a*) and the suture between tributaries B2a and B2b originate with patterns of reversed splaying crevasses (between stations 54, 55 and 65 in Figure 1). Such a pattern suggests lateral spreading around an obstruction to flow. Other shear margins begin with special crevasse patterns: packages of crevasses called the chromosomes in the case of the Heffalump, warps or buckles in the ice surface in the case of the Snake, and crossing crevasses in a pattern reminiscent of simple sketches of flying seagulls where flow splits into tributaries B1b and B2a. These patterns, and the reason for crevasses to appear in groups, are discussed by *Merry and Whillans* [1993]. Other special crevasse patterns have uncertain genesis. A discontinuous line of crevasses diagonally upglacier from the onset of the Dragon (starting at the right-hand edge of Figure 4*a* and angled diagonally up-glacier at about 45° to the flow traces) was mistaken as an extension of the Dragon (on the line between stations 71 and 65, Figure 1) by *Shabtaie and Bentley* [1988]. Its location with respect to bed topography [*Retzlaff et al.,* 1993] indicates that it relates to flow over a basal disturbance.

Subsurface Crevasses

A survey of the strain grid near UpB by short-pulse radar reveals two areas of crevasses that do not reach the surface [*Clarke and Bentley,* 1994]. A question is whether some of these crevasses are buried or whether they ever reached the surface.

One set of crevasses (which we call group I) very near the surface, is limited to the glacier-left part (viewing with glacier flow) nearest the shear margin (lines U, V, and X of the OSU strain grid, the southern portion of study in *Hulbe and Whillans* [1994]). This set appears to comprise buried examples of the type of crevasse that are visible at the surface up-glacier. The

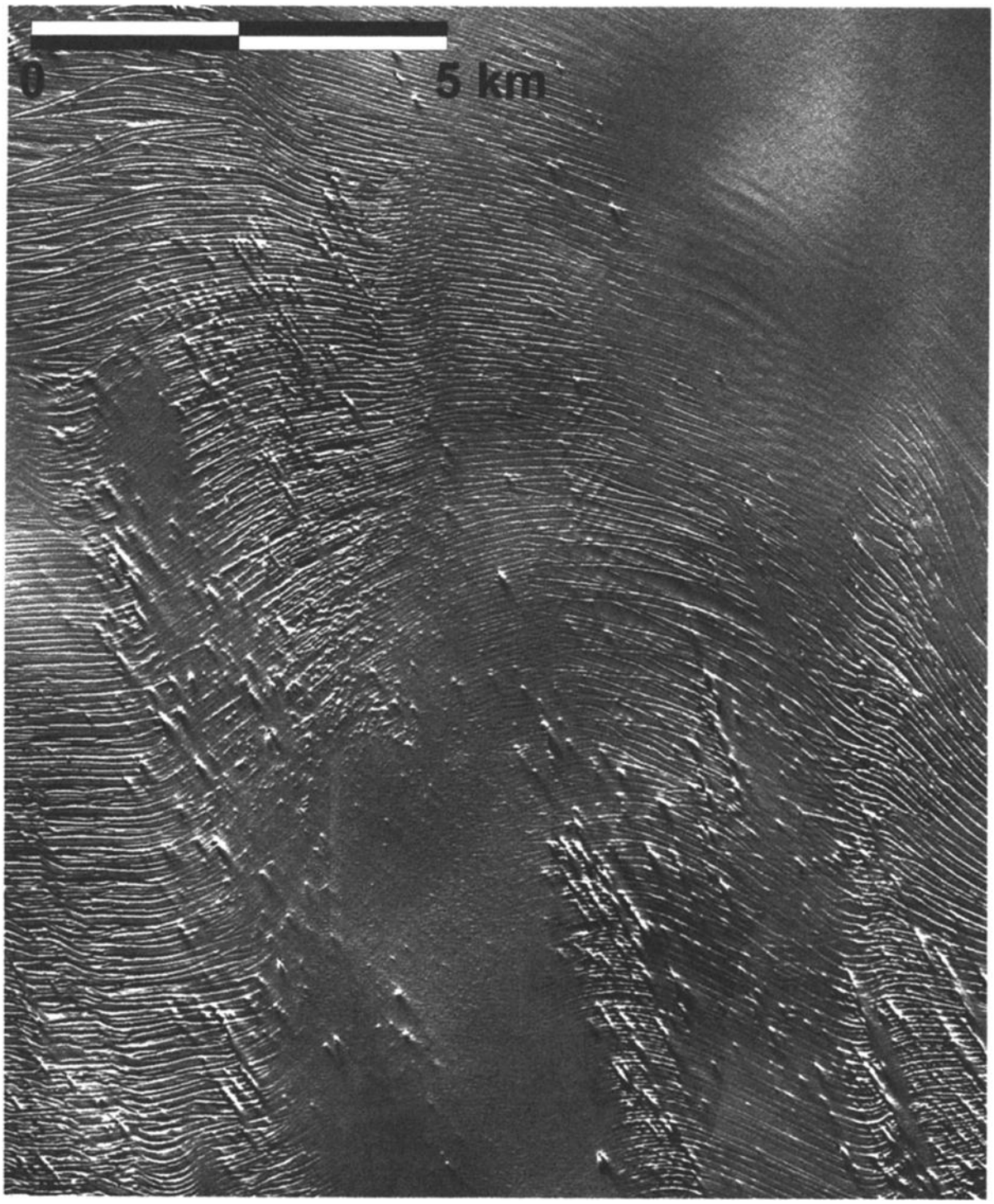

Fig. 4*c*. Subscene from Figure 4*a* showing oblique intersections of crevasses.

net rotation of these buried crevasses is greater farther from the glacier margin, as expected for steady flow because that ice has been in the ice stream longer and experienced more net rotation.

A second (group II) and deeper set of crevasses (deeper than 30 m) occurs beneath the first set and is also closer to the ice-stream centerline. The depth of the top of crevasses in this group is in snow strata about 200 years old (this is an age estimate if the crevasses reached the snow surface at formation). The down-glacial portion of this group (group IIdn) contains crevasses that are rotated by at least 45° out of alignment with present-day principal strain rates. Ice rotation rates vary within the region [*Whillans et al.,* 1993; *Hulbe and Whillans,* 1997], but a representative value is 1×10^{-3} a^{-1} (from the C line [*Hulbe and Whillans,* 1997]). With this rotation rate, the crevasse misalignment is achieved in 200 years (an accurate calculation would need to consider the crevasse-perpendicular rotation rate, but the result would be of similar magnitude). These calculations of crevasse depth and orientation are both consistent with the crevasses in this down-glacier group being some centuries old. Using present-day velocities, the nascent site for these crevasses must lie about 40 km up-glacier of the strain grid (typical speed of 200 m a^{-1}) – possibly at the very large crevasses just up-glacier of station 14 (Figure 1). The up-glacier members of this group (group IIup) are aligned perpendicular to the principal extending strain rates, suggesting a much younger age or ongoing formation – possibly at the crevasses closer to station 14.

The third region (group III) is at the kinematic centerline and no crevasses are detected by radar, consistent with typically smaller stress levels at the centerline. More important is the history of that ice. That ice must have passed glacier-right of the large crevasse field up-glacier of station 14.

Flow Traces

Active fast flow is marked by longitudinal ridges and furrows, called flow traces or flow stripes. They originate at disturbances to flow and the scar is carried off with the ice flow. The "suture" joining tributaries B1 and B2 is a prominent flow trace passing through stations 25 and 33 in Figure 1. Lesser flow traces originate within shear margins, such as the Heffalump [*Merry and Whillans,* 1993].

Flow traces have been used to define ice streams [*Hodge and Dopplehammer,* 1996; *Bell et al.,* 1998; *Stephenson and Bindschadler,* 1990]. Ice streams do contain flow traces, but flow traces also occur on outlet glaciers through the Transantarctic Mountains (e.g. figure 36 in *Swithinbank* [1988]) as well as on medium-speed ice in West Antarctica [*Bindschadler et al.,* 1996]. Flow traces originate far up-glacier [*Joughin et al.,* 1999] and can disappear down-glacier (e.g. at S80°20', W133°, in figure 4 of *Bindschadler et al.* [1996]; also noted by *Stephenson and Bindschadler* [1990]), presumably where velocity fluctuations within the inland ice or ice stream (figure 2 in *Bindschadler* [1993]) disrupt simple flow lines. The presence of flow traces can not be taken as a general diagnostic of ice stream flow, rather ice streams are defined here as grounded glaciers that are fast despite small driving stress (following *Bentley* [1987]).

Possibly flow traces are caused by strength variations in the ice, as found to be the explanation for the topographic features at UpB [*Hulbe and Whillans,* 1997]. Other suggestions are made by *Stephenson and Bindschadler* [1990], *Merry and Whillans* [1993] and *Gudmundsson et al.* [1998].

VELOCITIES

The most direct measurements of velocity have been obtained by leaving markers in the ice surface and surveying at least twice with ground-based satellite tracking. These velocities are depicted in Figures 1 and 3.

Speeds increase from about 300 m a^{-1} at the onset of ice stream flow to 865 m a^{-1} at the narrowest section and then decrease as the ice stream spreads onto the ice plain [*Whillans and Van der Veen,* 1993; *Bindschadler et al.,* 1993]. Here the 'onset' is taken to be at the site of major along-glacier decrease in driving stress despite fast speed. Distinct crevassed shear margins begin at about the same sites, where a speed contrast of about 100 m a^{-1} between potential ice stream and potential interstream ridge occurs over a distance of about 10 km or less (e.g. near stations 13 and 63 in Figure 1). The two main tributaries (B1 and B2) have very similar speeds, and join forming a suture across which there is very little shear. Sub-tributary B1b is slower and there is a shear zone where sub-tributary B1a fuses with it.

Spatially more dense measurements of velocity are obtained from feature tracking with repeat photography. A detailed map of speeds in the 10-block of tributary B2 (near the UpB camp) shows local longitudinal fluctuations of about 1% over 1000 m, and rather larger variability in the transverse component of velocity (figures 3b and 3d of *Whillans et al.* [1993]). *Whillans et al.* [1993] suggest that some of the fluctuations are due to rafts of stiff ice being advected along flow. A very precise survey of strains and vertical motions of a strain grid around the UpB camp leads to a further model for the fluctuations [*Hulbe and Whillans,* 1997]. Topographic features and the strain rate pattern in the ice stream are evolving with time. This result is interpreted as being due to tipped bands of crystallographically soft ice being advected along flow. This soft ice acts rather like soft fault gouge favoring lateral compression and growing topographic thrust-like structures (Figure 5). This discovery of strength heterogeneity accounts for the anomalous computation of reverse basal drag at certain sites [*Whillans and Van der Veen,* 1993]. That calculation was made under the assumption that there were no major horizontal gradients in ice strength. This advecting marbling or foliation of the glacier means that the flow of the ice stream is not steady on the time scale of advection of these features.

Two further blocks of feature tracking have been studied. Transects within each block have been stacked

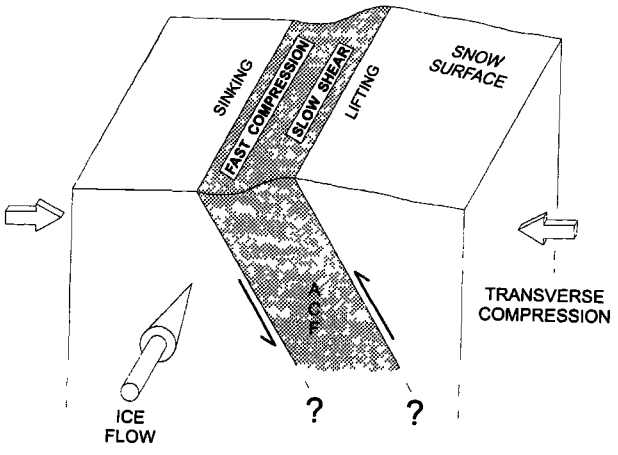

Fig. 5. Interpretation of the process leading to surface topographic variations on ice stream B. There is an inclined band of ice with a more intense crystal orientation fabric. This leads to zones of faster deformation and differential vertical motion [*Hulbe and Whillans,* 1997]. Reproduced from the Journal of Glaciology with permission from the International Glaciological Society and the authors.

to produce single width-scaled transverse profiles of ice speed (Figure 6, top panel). Speed is fastest near the centerline and decreases towards each margin. As developed in the appendix, the theoretical pattern for speed within the ice stream is a decrease as the 4^{th} power of distance from the center (taking basal drag, thickness, and surface slope constant across the section and using the usual constitutive relation). This pattern is followed in good approximation, notable exceptions being that the speed maximum in the 40-block is glacier right of the geometric center, and there are local fluctuations in speed.

Anisotropy

There is strong evidence for crystalline anisotropy in the ice from studies of seismic- and electromagnetic-wave velocities. Oblique-angle seismic reflection studies near UpB find that, through most of the ice thickness, the ice-crystal c-axes lie in or near the vertical plane normal to the flow direction of the ice stream and are distributed randomly within that plane [*Blankenship,* 1989]. This is corroborated by detailed radar-polarization experiments, which also find that the c-axes near UpB lie near the transverse plane [*Liu et al.,* 1994]. This fabric is one that might be produced by protracted simple lateral shearing.

The study of radar polarization also discovered a transverse change in the fabric over a horizontal distance of 100 to 200 m along a line some 15 km upglacier of UpB. The discontinuity lies within a few hundred meters of the crevasse-free zone near the kinematic centerline (as discussed under Subsurface Crevasses, above). This suggests that nearly all the ice of the ice stream, except that very close to the centerline, has developed a preferred crystal orientation fabric and that there are variations in the intensity of fabric.

The patch of 'soft' ice reported by *Hulbe and Whillans* [1997] (Figure 5) was not studied with radar polarization measurements so it is not proved that the two studies are finding the same type of feature. However, it seems reasonable to suppose that both found the same sort of important horizontal gradients in ice strength due to preferred crystal orientations within the ice stream.

Speed of Deep Versus Surface Ice

The net rate of vertical shear through the ice stream at three sites near the UpB camp has been measured by tracking basal radar diffraction patterns with time. The diffractions originate from irregularities at the base of the ice; shifts in the interference or fading pattern are tracked with repeated mapping at the surface [*Liu et al.,* in press]. The results are significantly different at the three sites. The deduced speed contrast between surface and bed (with one standard error uncertainties) are 1.0 (0.1), 0.1 (0.1), and -0.5 (0.1) m a^{-1} (the third site suggests faster deep ice). The down-glacier surface slopes are 0.0044, 0.0007 and 0.0031 and driving stresses are 40, 6 and 29 kPa, respectively. The variation may be due to flow in response to the local slope (and driving stress) or to shearing within 'weak bands' [*Hulbe and Whillans,* 1997]. The third site lies over such a weak band.

For the first site, the differential speed can be explained by lamellar ('laminar') flow in the vertical and longitudinal plane if basal drag equals two thirds of the local driving stress, that is 26 kPa. However, in light of the effects of other stresses and of strength inhomogeneities [*Hulbe and Whillans,* 1997], precise estimates of basal stress from such differential motion may not be possible.

MASS BALANCE

Early results of mass balance calculations indicate thinning of ice stream B [*Shabtaie and Bentley,* 1987; *Shabtaie et al.,* 1988; *Whillans and Bindschadler,* 1988]. Of these, the most data rich calculation finds that input in the catchment of the ice streams is 27% less than output from the mouth of ice stream B [*Whillans and Bindschadler,* 1988]. This translates to a mean thinning in the catchment at 0.06 m a^{-1}. Assessments of uncertainties indicate that the inherent spatial variability of accumulation rate limits mass balance determinations to about 7% confidence (standard error, divided by discharge) [*Venteris and Whillans,* 1998], and that the limits to uncertainties in catchment area are about 9% [*Price and Whillans,* 1998]. The southern boundary to the catchment of ice stream B is very poorly determined, so the real uncertainty in catchment area is larger, say 12%. The uncertainty in discharge is relatively small. Assuming that the errors in accumulation rate and in area combine statistically, as is common in mass balance calculations, leads to a standard error of

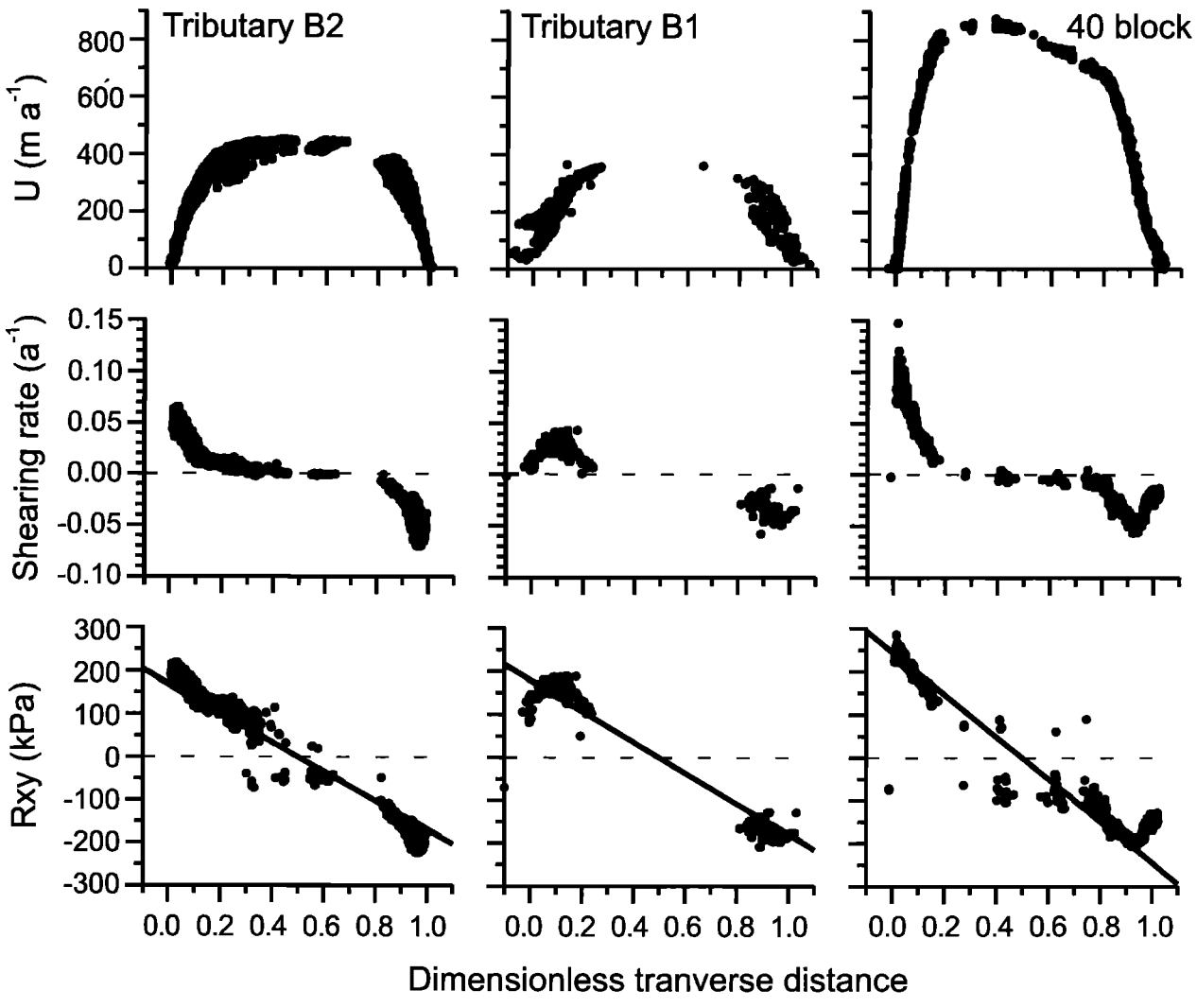

Fig. 6. For three cross-transects of ice stream B, longitudinal speed (top panels), lateral shearing rate (middle) and lateral shear stress (bottom). The lines in the bottom panels represent theoretical values if lateral drag opposes all of the action of the ice stream. Motion is toward the viewer. Transverse distance is scaled to ice stream width. [*Whillans and Van der Veen,* 1997]. Reproduced from the Journal of Glaciology with permission from the International Glaciological Society and the authors.

$(7^2 + 12^2)^{1/2}$ = 14% on the estimate of mass input to the ice stream system. Ice stream B together with its catchment is thinning at a rate that is two standard errors different from zero.

Shabtaie et al. [1988] compute a pattern of mass imbalance within the ice stream. The uncertainties allow for mass balances of zero. An uncertainty of 5% was assigned of the velocity profiles. This uncertainty is valid for the single velocity profile available at that time, at the mouth of the ice stream. Local fluctuations in ice speed are now known to be larger up-glacier (c.f. Figure 6). Modern uncertainties associated with mass balance calculations find that mass balances within ice stream B that are not different from zero.

Ice stream C is thickening in its lower and middle reaches (see *Anandakrishnan et al.* [this volume], for more detail). This is known because there is net accumulation of snow [*Whillans and Bindschadler,* 1988] and yet almost no discharge [*Whillans and Van der Veen,* 1993]. The feeding into the upper reach is moving at typical speeds (Figure 3). There is no major lateral ice divergence between these sites, so there must be a region of thickening between the upper and middle reaches. This pattern is confirmed by more recent work [*Joughin et al.,* 1999].

The coffee can method has been applied just outboard of the dragon at station 21 (Figure 1). It shows thinning at 0.096 (0.044) m a^{-1} [*Hamilton et al.,* 1998].

CHANGES WITH TIME

Non-traditional methods for detecting changes have demonstrated very important recent events. The evidence includes direct measurement of speed change with time on the ten-year scale, buried former ice streams and migration of shear margins. These results show that the ice streams are changing much more rapidly than classical glaciology, as used by *Whillans* [1982] for example, could permit.

Direct measurements of velocity and margin position show widening and slowing of ice stream B. Based on repeat velocity determination [*Stephenson and Bindschadler,* 1988] and on repeat satellite imagery [*Bindschadler and Vornberger,* 1998], the mouth of ice stream B is found to have been widening at 137 m a^{-1} and slowing by 2.4% a^{-1} since at least 1963. The upper reach of ice stream B is slowing by 0.7% a^{-1} [*Hulbe and Whillans,* 1997], and widening at 17 (6) m a^{-1}, based on crevasse shape with error estimate [*Hamilton et al.,* 1998], and at 7 m a^{-1}, based on temperature measurements [*Harrison et al,* 1998], and at 9.7 (1.1) m a^{-1}, based on repeat velocity determination [*Echelmeyer and Harrison,* 1999]. If these two sites are a reliable sampling, then the entire ice stream is slowing and widening.

Past changes in the ice streams are evident from peculiar surface forms and from buried features. The surface of interstream ridge A/B is lumpy, quite unlike the smooth surface of interstream ridge B/C (Figure 7, also *Bindschadler and Vornberger* [1990]). Ice speed is 12.6 m a^{-1} (Figure 1) on this interstream ridge, a typical value for an interstream ridge. The region has not been properly investigated, but the tentative interpretation is that it was formerly flowing faster, but has slowed down to form irregular highs and lows.

There are stranded shear margins. The interstream ridge between tributaries B1 and B2 (the Unicorn) contains a hook-shaped ridge (approximately joining stations 72 and 27 in Figure 1). This ridge is probably due to a buried old shear margin. The depth to subsurface crevasses in the northern part of the Unicorn indicates that the shear margin migrated gradually from the hook-shaped ridge, where it stood about 190 years before present, to the present position of the Dragon, which it reached about 130 years before present [*Clarke et al.,* in press]. There is an apparently similar stranded margin at the mouth of ice stream B [*Bindschadler and Vornberger,* 1990]. These two samples suggest that the ice stream was wider in the past and became narrower. The measurements noted above indicate that the sense of width change is now reversed.

Ice stream C, the next ice stream north, was also active, but its middle and lower reaches are now nearly inactive (Figure 3). Proof of former activity is the existence of subsurface crevasses [*Robin et al.,* 1970; *Rose,* 1979; *Bentley et al.,* 1985]. These crevasses probably once reached the surface, especially near the lateral margins, so the depth of burial indicates a time of about 140 years (corrected for the decade that has elapsed since the measurements) [*Retzlaff and Bentley,* 1993; *Bentley et al.,* in press] since the activity ceased. The up-glacial portion is traveling at 'normal' speeds for ice feeding into an ice stream (Figure 3). There must be a growing bulge near longitude W135°.

BED MOBILITY

Seismic wide-angle reflection experiments at UpB in 1983-84 obtained both compressional-wave (P-wave) and shear-wave (S-wave) reflections not only from the base of the ice, but also from a second reflector a few meters deeper [*Blankenship et al.,* 1986, 1987]. Such dual reflections from each of two layers have not been obtained elsewhere on the ice streams, despite attempts at DnB and UpC and in later years at UpB. For data from 1983-84, inversion of reflection times yields determinations of the P- and S-wave velocities in the subglacial sedimentary layer, showing that the porosity of the sediments is about 0.4 and that the effective pressure is only about 50 kPa (the ice overburden is 9000 kPa). These numbers indicate that the sediment, presumed to be glacial till, is dilated, water-saturated, and very weak, characteristics that are confirmed by drilling to the bed [*Kamb,* this volume; *Engelhardt and Kamb,* 1998].

Extensive seismic reflection profiling reveals that the subglacial sediment layer is widely distributed near the UpB camp. The average thickness is 6 to 7 m [*Rooney et al.,* 1987]. The upper surface of the layer is smooth, but the lower surface is fluted parallel to ice-stream movement. These sediment-filled flutes are as much as 13 m deep and 1000 m across. In one or two locations the sediment is no thicker than the resolution of the seismic experiments (about 2 m), so it may pinch out entirely. Nowhere on the reflection profiles is any feature discerned to penetrate more than a few meters into the ice from the bed. The bed is smooth as well as soft.

The presence of soft, deformable, dilated subglacial sediment (probably till) opens up the possibility that debris has been, and presumably still is being, transported with the glacier or with subglacial water motion. The best evidence for till deposition is the discovery of a feature similar to a delta beneath the mouth of ice stream B [*Shabtaie and Bentley,* 1987] and seismic evidence for foreset beds within it [*Rooney,* 1987].

There is little information on the time scale for deposition of this delta-like feature. It could be forming at present or it could be a relict from a time of adjustment of the ice sheet, for example to the rise in global sea level 8000 years ago. A change in configuration of the ice would lead to excavation of many soft deposits that had accumulated in up-glacial basins. That is, debris transport could be continuous or episodic and it is not known what the current phase of activity may be. However, some debris must be in traction today, if only due to the effect of roughness elements (on the order of 1 m in size, as deduced from radar diffraction studies) that must be plowing the bed.

Other Features of the Bed

There are glacier-parallel stripes in bed character as deduced by mapping acoustic impedance using the phase of P-wave reflections under ice streams B and C

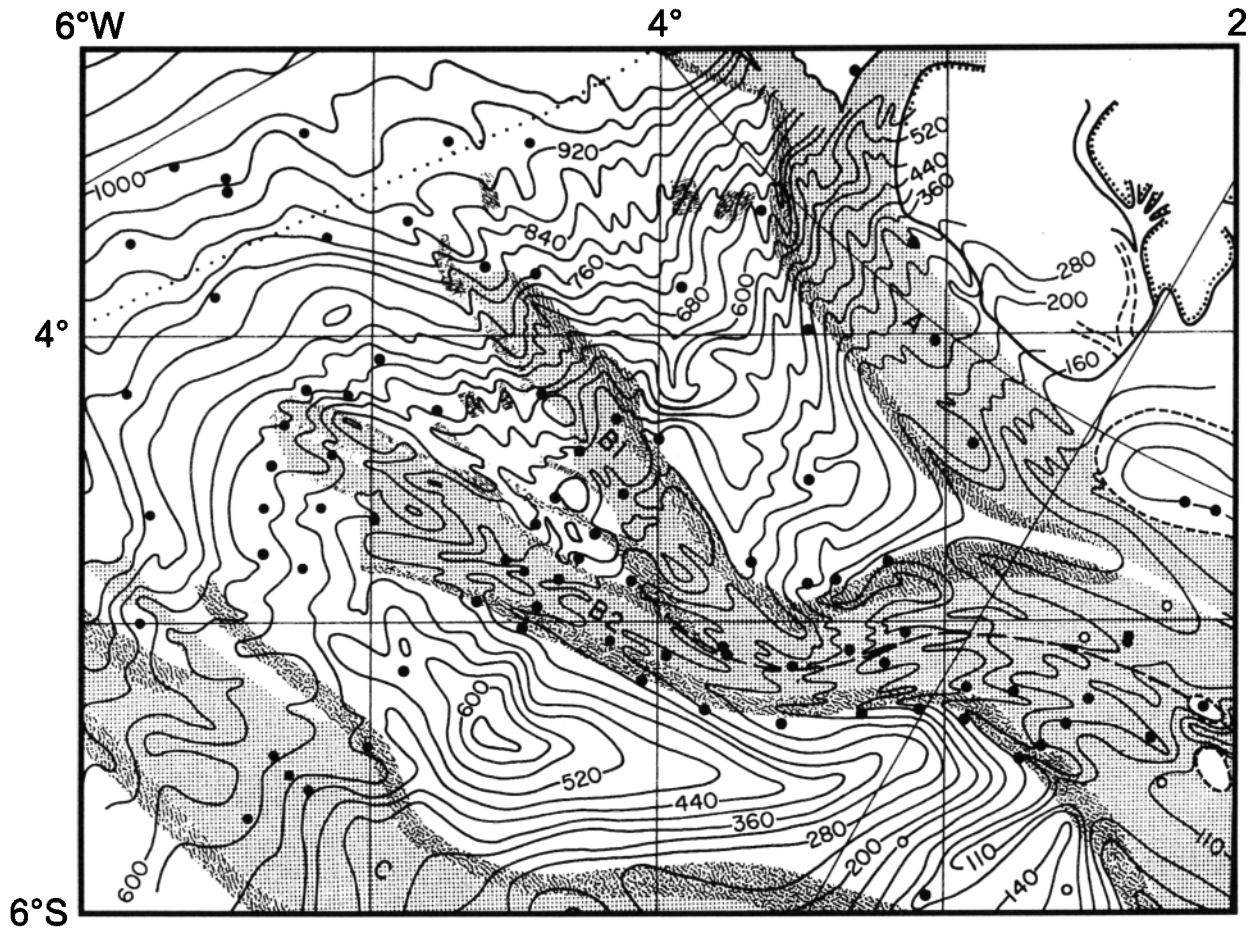

Fig. 7. Elevation contours of ice stream B and neighboring regions. Dots represent survey stations used for elevation control, many of which appear in Figures 1, 2 and 3. Squares are about 110 km on a side. [*Shabtaie et al.*, 1987].

[*Atre and Bentley,* 1993, 1994]. Because estimated impedances in a dilated bed (porosity 0.4) and in the lowermost ice are very nearly the same, minor differences in the nature of the sediments composing the bed, or the physical state of the bed (e.g. the porosity) can change the impedance contrast. Lateral variations of this kind provide an explanation for the relatively high impedances found in some places beneath ice stream B. Under ice stream C, the bed beneath the faster flowing (10 m a^{-1} at station 90 in Figure 3) ice with surface flow traces (in satellite imagery, [*USGS,* 1992]) has a low-impedance bed (consistent with higher-porosity subglacial sediments), whereas that under the very slow (2 m a^{-1} at stations 80 and 82 in Figure 3) ice showing a mottled surface in satellite images has a relative higher-impedance bed (consistent with more bed strength).

Basal stripes are evident in radar as well. Near UpB the basal echo strength varies slowly in the direction of ice motion and rather more in the transverse direction (Figure 8). The transverse scale of variation is some 10 to 20 m. There is a longer 150 m scale as well in transverse variation [*Novick et al.,* 1994]. The bed contains flow-aligned stripes of differing bed type.

Microearthquake studies have yielded evidence of sticky spots (sites of concentrated basal drag) beneath both ice streams [*Anandakrishnan et al.,* this volume]. However, the analysis of the pattern in ice velocity across the full width of ice stream B (next section, Figure 6) finds no dynamically important concentrations of friction, meaning that the earthquake-determined sticky spots do not provide a significant restraint to the flow of ice stream B.

Folding of the internal structure of ice streams has been sought with detailed radar work. In most places, radar-reflecting internal layers are continuous. At UpB they are parallel to the surface in the flow direction but show divergence from the surface in the transverse direction [*Schultz et al.,* 1987]. Near the mouth of ice stream B and within ice stream C there are transverse folds in the internal layers, and the axial planes are tilted

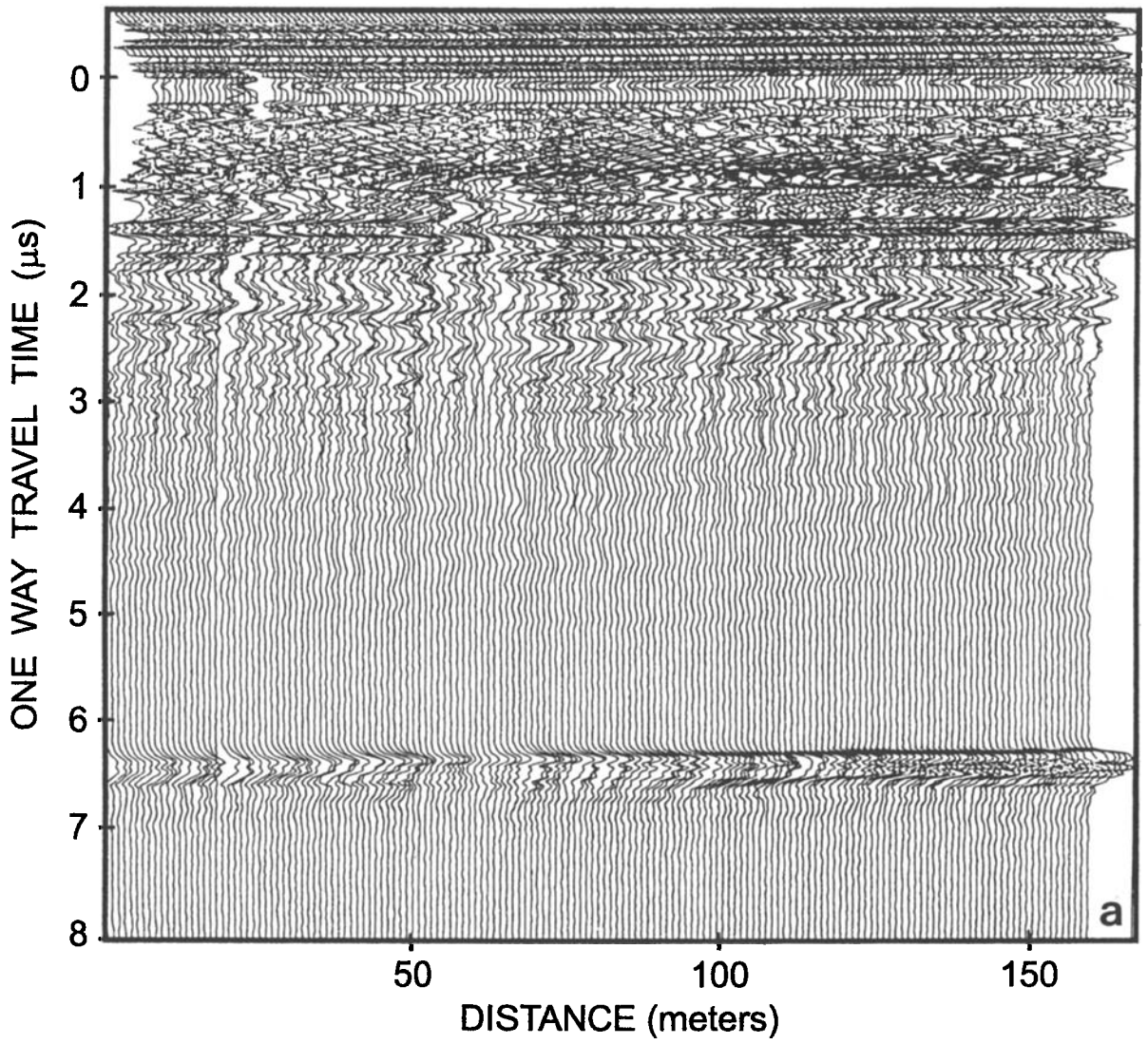

Fig. 8. Stacked radio-echo traces from near the UpB camp. Part a is a transverse transect showing that bed returns fluctuate over horizontal distances of 10 to 20 m. Part b is a longitudinal transect showing that bed variations have a much longer scale length. [*Schultz et al.*, 1987]. Reproduced from the Annals of Glaciology with permission from the International Glaciological Society and the authors.

variously up- and down-glacier [*Jacobel et al.*, 1993; *Jacobel and Grommes*, 1994]. These must indicate a temporally and spatially varying basal drag somewhere up-glacier. It may be a similar phenomenon to the thrusting discovered near the UpB camp [*Hulbe and Whillans*, 1997].

Conditions under the inactive ice stream C have been investigated by several techniques that are discussed by *Anandakrishnan et al.* [this volume]. Most of the bed is soft and wet; in some places the water layer may be at least several centimeters thick.

The simple extension of the finding at both UpB and UpC that basal water is nearly at overburden pressure [*Kamb*, this volume] is that water should flow at the ice-bed interface and collect according to the relief on the bed and pressure gradients due to ice thickness gradients. On the ice streams, the basal hydrologic gradient is dominated by surface slope, bed slope being secondary. Water flow according to the surface topography leads to divergence and convergence in the expected subglacial water flow lines and so to regions without a water supply, presumably a sticky spot to ice sliding, and to subglacial ponds. However, the maps of basal radar echo strength do not correlate with the likely distribution of subglacial water [*Novick et al.*, 1994]. Other considerations affect basal reflection strength; possibly basins filled with sediment affect the radar in the same way as water-filled ponds. However, the

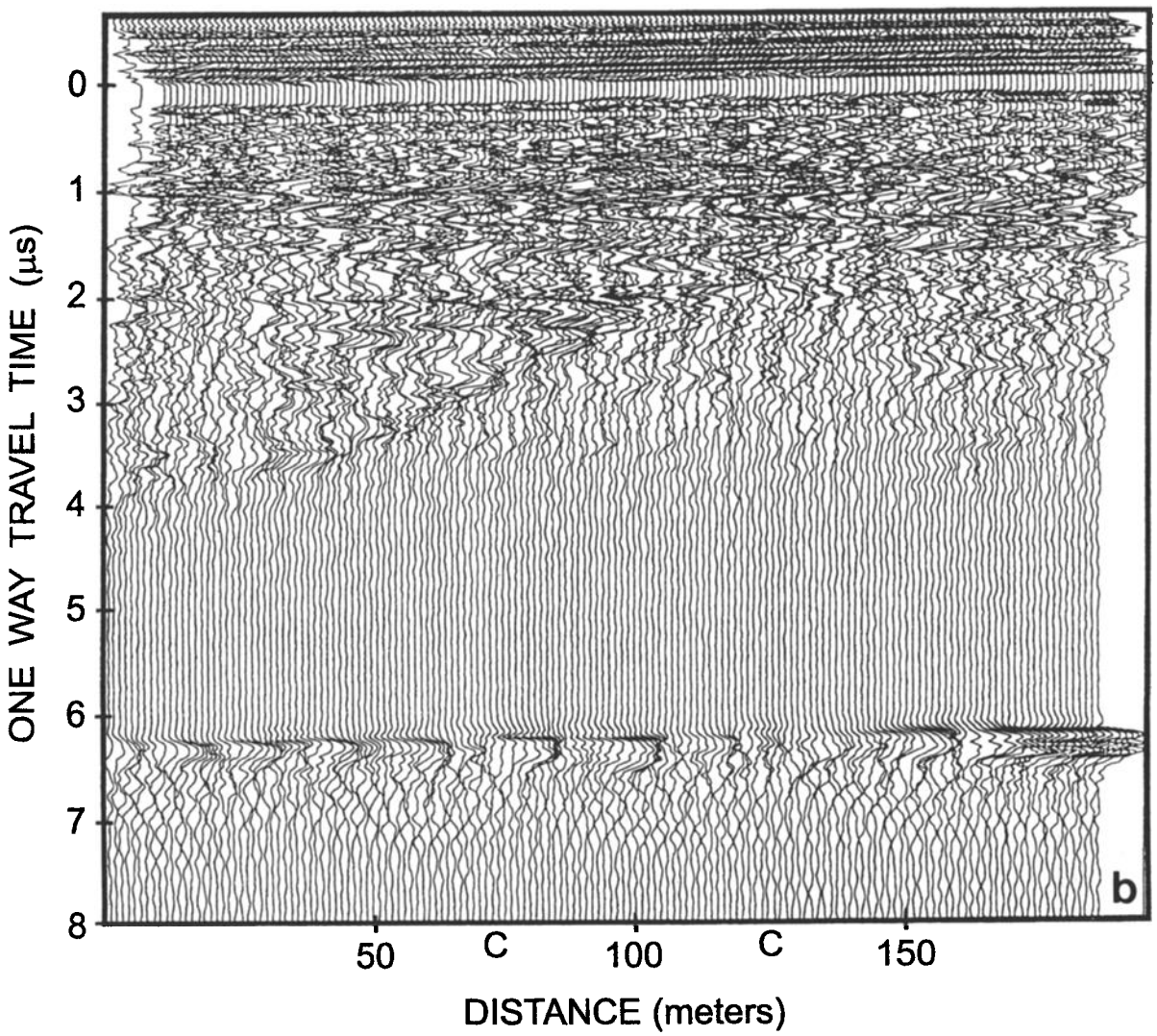

Figure 8. Continued.

straightforward interpretation is that water collection does not seem to be a factor in bed character.

The contrast between the beds of ice streams B and C and the intervening interstream ridge is addressed with an analysis of the strength of airborne-radar echoes from the downstream ends of ice streams B and C [*Bentley et al.*, 1998]. Returns from beneath interstream ridge B/C are weaker than those from the base of the ice streams, most probably because the interstream ridge is frozen to its bed. Returns from the bed of ice stream C are bright, in many places brighter than those from ice stream B. The beds of both ice streams are probably wet. The cause for brightness variations within ice stream C is not known, but suggestions are that there is trapped seawater, or that some other property of the bed affects reflection strength, or that there are variations in the amount of energy lost by scattering from subsurface crevasses.

FORCE BUDGET

The gross-scale mechanics controlling glacier flow are assessed by evaluating the action effect of gravity, the driving stress, and the potential reactions. The reactions or resistance can come from the bed, from the sides or from the ends of the glacier section being considered. Driving stress is calculated from the geometry of the glacier. Net resistances from along the glacier or from the sides are assessed from measured strain rates using the constitutive relation for ice to obtain stresses. Basal resistance is deduced as the residual in the calculation needed to balance forces.

The general formula for force budget may be expressed for a unit of map area [*Van der Veen and Whillans*, 1989, equation 14]:

$$\tau_{dx} = \tau_{bx} - \frac{\partial}{\partial x} HR_{xx} - \frac{\partial}{\partial y} HR_{xy} \qquad (1)$$

In this case the forces in the down-glacier x-direction are considered. The action or driving stress is on the left-hand side and the terms on the right hand side are, respectively, basal drag, differential longitudinal tension and differential lateral drag. Resistive stresses, represented by R, are thickness means and they are estimated from strain rates.

Action of Gravity

Glacier motion is driven by gravity as described by the driving stress, τ_{dx}, being the horizontal action per unit map area. It is calculated from the product of surface slope, $\partial h / \partial x$, and ice thickness, H:

$$\tau_{dx} = -\rho g H \frac{\partial h}{\partial x} \qquad (2)$$

in which, ρ and g represent ice density and acceleration due to gravity, respectively. In practice, the most critical quantity is surface slope because it varies by large factors. The driving stress along ice stream B is depicted in Figure 2, 3rd panel.

Longitudinal Tension / Compression

The longitudinal term, $\partial HR_{xx} / \partial x$, is evaluated from measurements or assessments of longitudinal and transverse stretching rates together with the constitutive relation for ice. Longitudinal stretching is computed from measurements of velocity along the ice stream centerlines:

$$\dot{\varepsilon}_{xx} = \frac{\partial U_{max}}{\partial x} \qquad (3)$$

It is depicted in Figure 2, 5th panel. Transverse strain rate is evaluated from longitudinal variations in ice-stream width, W, as shown in Figure 2, 2nd panel:

$$\dot{\varepsilon}_{yy} \equiv \frac{\partial u_y}{\partial y} \cong \frac{U_{max}}{W} \frac{\partial W}{\partial x} \qquad (4)$$

in which the simplification is made that the centerline speed can be substituted for the width mean. This is not a necessary simplification, but one learns *a posteriori* that the accuracy of transverse strain rate is not critical to the analysis of force budget. Longitudinal tension is calculated from these strain rates using the constitutive relation [*Hooke,* 1981]:

$$R_{xx} = B \dot{\varepsilon}_e^{-2/3} [2\dot{\varepsilon}_{xx} + \dot{\varepsilon}_{yy}] \qquad (5)$$

The rate factor, B= 540 kPa $a^{1/3}$ is obtained from the values presented by *Hooke* [1981] and the depth-temperature profile at UpB [*Engelhardt et al.,* 1990]. As is usual, the exponent in the flow law is taken to be 3. In evaluating the effective strain rate, $\dot{\varepsilon}_e$, vertical shearing is neglected. This is appropriate in the analysis of the budget of forces because most vertical shearing occurs in deep ice. This warm ice is not strong and so does not carry large horizontal stresses, R_{xx} and R_{yy}. Vertical normal strain rate is obtained from horizontal strain rates by invoking incompressibility. The expression used for effective strain rate is

$$\dot{\varepsilon}_e = [\dot{\varepsilon}_{xx}^2 + \dot{\varepsilon}_{yy}^2 + \dot{\varepsilon}_{xx}\dot{\varepsilon}_{yy} + \dot{\varepsilon}_{xy}^2]^{1/2} \qquad (6)$$

Lateral shear strain, $\dot{\varepsilon}_{xy}$, varies across the ice stream. At the kinematic centerline its value is zero. The tensile stress so computed for the centerline is displayed in the 6th panel of Figure 2. The pattern in R_{xx} is nearly the same as the pattern in longitudinal stretching, $\partial U_{max} / \partial x$, from which it is mainly derived.

Tensile stress, R_{xx}, is large (about 150 kPa) along most of the ice stream (6th panel of Figure 2). It evokes the vision that ice streams are pulling ice out of the interior ice reservoir [*Hughes,* 1998]. However, it is the longitudinal gradient in tension that is important to the budget of forces. This is displayed in the last panel of Figure 2, as $\partial HR_{xx} / \partial x$. Compared to driving stress, τ_{dx}, which is 10 kPa or more, longitudinal tensile gradients are small (5 kPa or nearer zero). Differential longitudinal tension is a minor player in the balance of forces all along ice stream B.

There is a short reach within tributary B2, just up-glacier of the UpB camp, where tension is smaller than for most of the rest of the ice stream. This reduced tension would mean fewer exposed crevasses, and indeed the UpB camp area is the only place on the middle reach of ice stream B where large aircraft could land safely. The small tension is a consequence of the more nearly constant speed in this reach. That in turn is due to the more nearly parallel sides and nearly constant thickness of the ice stream. The gradient from small tension at UpB to larger tension down-glacier leads to the biggest value in longitudinal force gradient for the ice stream (Figure 2, last panel).

Near the ice shelf, tension drops to near zero, then becomes slightly negative. This small value of R_{xx} means that there is very little stress transmission between the ice shelf and ice stream.

Buttressing Force From the Ice Shelf

It was once a common view that the ice shelf may be holding back the grounded ice sheet [*Jenssen et al.,* 1985, page 2; *Bindschadler and Vornberger.,* 1990; *MacAyeal,* 1989]. Measurements at the mouth of ice stream B show that the longitudinal resistive stress is nearly zero (6th panel in Figure 2 at x = 100 km). The contribution of the ice shelf to the budget of forces for the ice stream is negligible because the ice shelf is thin and stresses are small. Should sea level or ice thickness near the flotation point change then there would be a change in the area and maybe value of basal drag for the

ice stream, most likely an along-glacier migration in flotation position. Some scientists suggested other patterns in reaction, including strong longitudinal stresses and longitudinal stress gradients. The simpler model would retain the current pattern in force transmission.

A change in any one part of the system, such as reduction of ice shelf, must eventually propagate along glacier to affect other parts, but is as yet undemonstrated with observation. There is evidence for down-glacier propagation of disturbances in the Ross Ice Shelf [*Casassa et al.,* 1991]. None is definitively reported as of yet for up-glacier propagation, although *Retzlaff and Bentley* [1993] suggest that a wave of stagnation moved up-glacier from the mouth of ice stream C. The Holocene rise in sea level must have affected the ice sheet in such a sense.

Tension From the Inland Ice

Another suggestion has been that the ice streams may be pulling away from the inland ice ("pulling power" [*Hughes,* 1998, pages 51 and 110]). Speeds do increase down-glacier at the onset to ice-stream flow (Figure 2, 5th panel), implying longitudinal tension (6th panel). However, the gradient in this tension is very small (bottom panel), indicating that it plays a small role in ice stream dynamics. *Hughes* [1998, pages 51 and 166] suggests that there is an arc of "primary transverse crevasses across the head of ice streams." There is no such arc for ice stream B (Figure 4*a*). As shown in the lowest panel of Figure 2, the tendency for ice streams to pull ice out of the inland ice reservoir is minor.

However, as with ice-shelf buttressing, the onset region is part of a linked system. Should for some reason the ice streams be removed there would be up-glacially propagating effects.

Lateral Drag

Drag from the sides is estimated from measurements of lateral shear strain rate and used with the constitutive relation to compute lateral shear stress. The first results come from a line of poles surveyed across the Dragon, near UpB [*Echelmeyer et al.,* 1994; *Harrison et al.,* 1998]. Further data come from the repeat photogrammetry of three sections across the ice stream. Figure 6 shows lateral shearing rate and the computed shear stress. Lateral drag varies continuously and nearly linearly from one side of the ice stream to the other, meaning that there are no major sticky spots. The line in Figure 6 (3rd row of panels) represents the stress necessary to oppose the action of gravity (as developed in the appendix). The inferred stresses do balance, or more than balance the gravitational driving force.

Jackson and Kamb [1997] provide an explanation for the apparent overbalance. Working with ice samples recovered from the ice stream they determine that ice from the shear margin is weaker than isotropic ice because of a special crystal orientation fabric. Allowing for this effect brings the calculated stresses in Figure 6 close to the theoretical solid line, removing the discrepancy. Moreover, the stress required to deform the ice samples at the measured rate accords with the inference from the full transect.

The dominance of lateral drag applies at the mouth of ice stream B as well [*Bindschadler et al.,* 1987]. There, 83% (standard error: 18%) of the driving force is opposed by lateral drag [*Whillans and Van der Veen,* 1997].

Differential lateral drag, $\partial HR_{xy}/\partial y$, is linked with centerline speed, U_{max}, and ice stream width, W (appendix). The result is displayed in Figure 9 (middle panel). It is about 10 kPa, and that is enough to oppose most of the driving stress within the ice stream. Up-glacier of about x = -100 km, lateral drag plays a much smaller role.

Basal Drag: Variation Across the Ice Stream

Basal drag is computed as the residual of the sum of driving stress, longitudinal force gradients and lateral drag. The residual computed in this way is very small, being some 0 to 7 kPa, for each of the sections of ice stream B that have been studied (Figure 6). Basal drag is small right to the edge of the ice stream (match of points to line in Figure 6; also *Echelmeyer et al.* [1994]). This raises the difficult question of what is responsible for such small friction despite ever decreasing speeds toward the margin (and large basal friction at the outboard margins).

Basal Drag: Variation Along the Ice Stream

Supposing that the three transects of Figure 6 are representative of the entire ice stream, the procedure in the appendix is used to compute basal drag all along ice stream B (Figure 9, bottom panel).

Up-glacier of x = -100 km, basal drag is large and about equal to the driving stress. Lateral drag and longitudinal force gradients are not important. This is much as has been found elsewhere on inland ice when averages are taken over spatial scales of 20 km or more (*Whillans and Johnsen* [1983] for Byrd Station, Antarctica; *Whillans and Jezek* [1987] for Dye3, Greenland).

Down-glacier of x = -100 km, basal drag is much smaller, in fact nearly zero. Lateral drag takes up the dominant role, becoming important where basal drag decreases.

A concern has been that the findings on basal water flow and storage and of ice friction near UpB may not be representative for the ice stream as a whole. There are fewer exposed crevasses near UpB than elsewhere on the ice stream. Maybe the reasons for fewer crevasses are also reasons to suspect that basal conditions are unusual. The reason for the paucity of exposed crevasses is now known to be mainly because longitudinal stretching is smaller than elsewhere, being about 2×10^{-3} a^{-1} at UpB [*Hulbe and Whillans,* 1994] as opposed to 4×10^{-3} a^{-1} over the long reach between the UpB camp and the narrows at station 33 (Figure 1). The smaller rate of stretching means that crevasse bridges do not fail at UpB. The reason for smaller

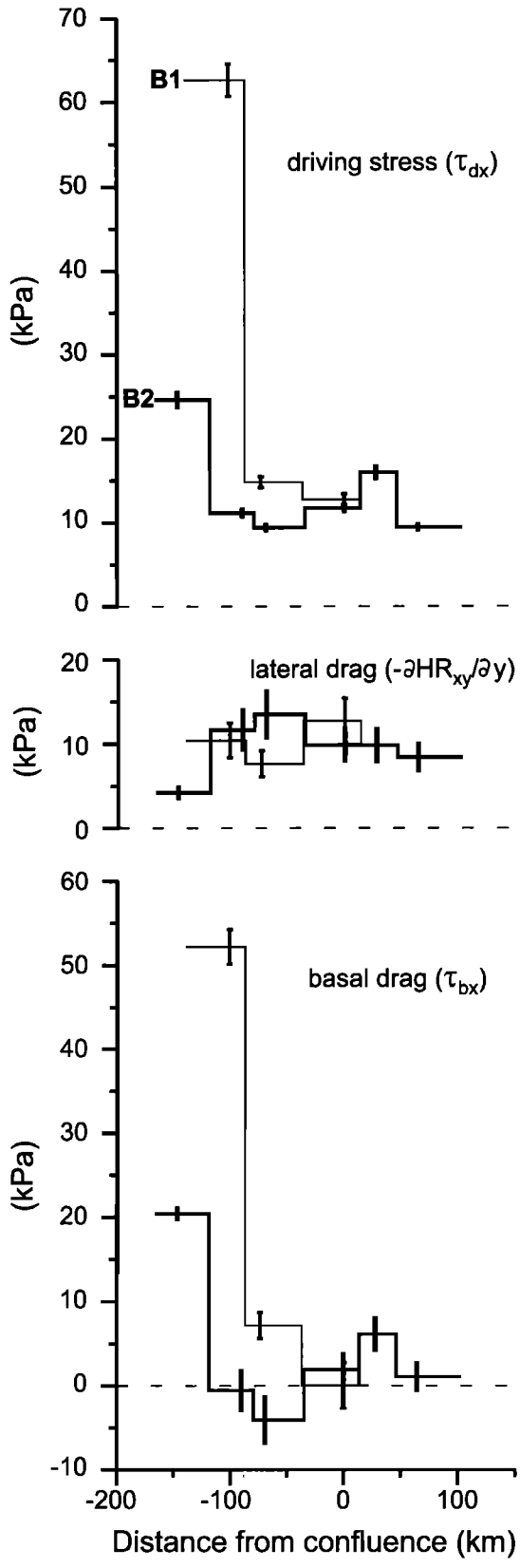

Fig. 9. Components in the budget of forces along ice stream B. Driving stress is repeated from Figure 2, with uncertainties that trace approximately equally from surface elevation (standard error: 2 m) and thickness (50 m). The uncertainty in lateral drag, $\partial HR_{xy}/\partial y$, derives mainly from uncertainty in the value of B, with values in the range 400 to 750 kPa $a^{1/3}$ considered. Basal drag is computed from the sum of the terms above, with a small contribution from longitudinal force gradient from Figure 2.

stretching is that the ice thickness increases downglacially [*Novick et al.,* 1994] and there is only a minor narrowing of ice stream width [*Whillans et al.,* 1993]. Nevertheless, crevasse density is large [*Clarke and Bentley,* 1994], it is just that fewer crevasses reach the surface. The measured patterns in velocity for other studied sections of ice stream B differ from each other as much as from the section at UpB, so there does not appear to be anything especially unusual about the UpB camp region. This means that the results of studies near the UpB camp are probably representative of most of the ice stream.

Velocity gradients on the nearly inactive reaches of ice stream C are too small (Figure 3) for horizontal force transmission to be significant beyond the scale of about 5 km. At that scale basal drag balances driving stress.

ONSET

Using the definition of the onset to be where driving stress decreases and speed increase along glacier, the onset is at x ≈ -100 km, the empirical finding is that

up-glacier of the onset:

$$\tau_{dx} = \tau_{bx} \approx 20 \text{ to } 70 \text{ kPa; speed} < 300 \text{ m a}^{-1}.$$

down-glacier of the onset:

$$\tau_{dx} = \partial H\bar{R}_{xy}/\partial y \approx 10 \text{ kPa; speed: } 300 \text{ to } 800 \text{ m a}^{-1}.$$

A very simple picture emerges from this study. For the inland ice, basal drag is at normal levels for an ice sheet [*Drewry,* 1983], in the range 20 to 70 kPa, and the large-scale balance of forces is between gravity (as described by the driving stress) and the bed. At the ice-stream onset, basal drag decreases to values of 0 to 5 kPa, and the large-scale balance of forces is between gravity (which generates a driving stress of about 10 kPa) and the ice-stream sides. Basically, basal drag is large under inland ice, but is nearly zero under the ice stream and mechanical control changes from the bed, under inland ice, to the sides, within the ice stream.

There are no distinct topographical steps that delimit the transition from inland-ice flow to ice-stream flow at the head of the ice streams. For example, the beginning of ice stream B2 and its shear margins, the snake and dragon, start at a nearly level bed, and the beginning of ice stream B1b, and its shear margin, the Heffalump, begins with a small upward step.

Other definitions of the onset lead to:

x = -400 km: steeper slope [*Bell et al.,* 1998].

x = -400 km: lateral shearing [*Anandakrishnan et al.,* 1998].

x = -100 km: first crevasses in a shear margin (Figure 1).

x = -310 km: first flow traces [*Hodge and Dopplehammer,* 1996; *Scambos and Bindschadler,* 1997; *Bindschadler and Vornberger,* 1990].

x = -200 km: most up-glacial crevasse [*Bindschadler,* 1997].

Most of these other definitions imply longer ice streams than the definition used here.

HYPOTHETICAL CONTROLS

A central need is to understand the physical reasons for ice streams and their changes with time. From their first discovery, hypotheses have been advanced to account for the ice streams and their changes. Not all the hypothetical explanations are mutually exclusive and competitive with one another. It is possible that several hypothesized processes can operate at once. As with other branches of science, the glaciological community has devised tests to seek to disprove various hypotheses. The endeavor has been very successful, and the range of feasible processes has been considerably reduced. A large number of hypotheses have been advanced for the behavior of ice streams. Here we review each of them.

Basal Heat Feedback

One of the first models for the behavior of ice streams is that the faster the ice moves the more work is expended as basal heat and the more heating or basal melting is produced. Basal heat can raise the temperature to melting and basal water can allow sliding and lubricate the flow. This model is still attractive.

Calculations of basal heating support this model [*Rose,* 1979]. The motion of the ice stream is taken to be opposed by friction at the bed, and although the driving stress of an ice stream is small, the speed is so fast that heat production (the product of driving stress and speed) is much more than for inland ice. This heat input may keep the ice streams active.

Using this model *Payne* [1998] is able to numerically reproduce fast ice streams on wet beds separated by nearly stagnant interstream ridges that are basally frozen. The location of ice streams corresponds with actual ice streams. There are two major observational discrepancies with the model. First, the interior of the ice sheet at Byrd Station is predicted to be basally frozen, yet observations find it and the region around it to be wet based [*Ueda and Garfield,* 1970; *Whillans and Johnsen,* 1983]. Second, the lower and middle reaches of ice stream C are predicted to be nearly stopped on account of being basally frozen, yet the bed is largely wet [*Shabtaie et al.,* 1987; *Bentley et al.,* 1998]. One explanation for the discrepancies is that Payne selected a very small value for geothermal heat flow. Should a more common value [e.g. *Sclater et al.,* 1980] be selected, then the wet-based conditions would be calculated to be more pervasive, as observed, and not so narrowly confined to ice streams. Payne uses the model to describe time changes in ice streams. It is not demonstrated that such changes would occur with a more common value of geothermal heat flow. Possibly this model can explain frozen beds under interstream ridges, but further processes must be invoked to explain the positions of ice stream onsets.

Basal heating may explain abrupt change in speed at the sides of the ice streams (e.g. Figure 6). *Jacobson and Raymond* [1998] introduce the concept of an "edge shield" in which heat dissipation in the ice of the shear margin raises its temperature and reduces the vertical temperature gradient and upward heat conduction. With this edge shield, geothermal and frictional heat cannot be conducted upward as rapidly as otherwise. This leads to wet-based conditions under the shear margin, but not under the interstream ridge. There is a possible feedback between the generation of an edge shield, or warmed margin, and the time evolution of the position of the shear margin.

A second version of this model argues that the water produced lubricates the motion. The more water production the more potential lubrication. Ice stream C may have shut down because the lubricating water stopped being produced in sufficient quantity. That is, the ice stream did not necessarily freeze to the bed, it is just that the lubrication ceased to be sufficiently thick.

A third version of the model emphasizes water flowing in from up-glacier. The critical question concerns how this water flows, as a film, in wide shallow canals, or in narrow channels and whether the flow style can change. More widely distributed lubrication leads to smaller basal drag and faster ice speeds. Drawing on models for automatically surging valley glaciers, most particularly Variegated Glacier, Alaska, U.S.A., raises the suggestion that the behavior of the ice stream system is linked with instabilities in basal lubrication, although perhaps without generation of a full surge cycle. *Retzlaff and Bentley* (1993) suggest that the stagnation of ice stream C involved a drop in water pressure at the bed due to a conversion from water flow as a sheet to channelized water flow.

All three versions of the model of basal heat balance deserve fresh visits. The discovery that basal drag under ice streams is very small means that there is less heat production than earlier supposed. Following a flowline from inland ice to the ocean, one would find a maximum in basal heat production near the ice stream onset, where driving stress is large and opposed by friction at the bed and ice speed is large. Within the ice stream, speed is very large but basal drag is very small, but the combination can still lead to significant heat dissipation at the bed [*Van der Veen and Whillans,* 1996]. However, the way that basal drag and speed can change together with ice-stream evolution is not clear. Perhaps water can freeze on and consume available basal water under ice streams. This process could eliminate the lu-

brication and eventually cause an increase in basal drag under the ice stream and reduce speed.

Piracy

Rose [1979] proposes that ice stream B is capturing the catchment area of ice stream C. Inland ice feeding into ice streams B and C separates in a region with very small surface slope. The direction of driving stress is not clear, and there could be an ongoing shift in flow line direction. That is, flowlines that formerly were directed down ice stream C are now shifted toward ice stream B. However, this vision of the time evolution of the pair of ice streams is not compatible with measured velocities at the head of the ice streams.

The ice feeding into ice stream C is behaving normally (Figure 3; *Anandakrishnan and Alley* [1997]). In fact, velocities are fast for such a small driving stress and are directed down ice stream C. This reach is either an active ice stream or very nearly so. Such velocities disprove the ongoing ice-piracy model.

A variant on the piracy model is that it is rerouting of subglacial water that initiates the switches in behavior. Gradients in basal hydrologic potential are so small at the head of ice stream C that it is not clear which route is taken by the subglacial water from under much of the inland ice. *Alley et al.* [1994] and *Anandakrishnan and Alley* [1997] propose that there has been a switch, that water once descending ice stream C now crosses beneath interstream ridge B/C and then descends ice stream B. The result is that water supply to the middle and lower reaches of ice stream C has been cut off, reducing lubrication and slowing ice stream speed.

This model depends on the validity of the hypothesis that an up-glacier supply of basal water is needed to maintain fast flow. It also requires that the rerouted water cross beneath an interstream ridge without causing fast ice motion of the ice above. Perhaps the water passes beneath the interstream ridge in a narrow channel. A further idea is that the piracy model applied in the past and that since then the upper reach to ice stream C has thickened. Such a thickening may make such past piracy difficult to demonstrate.

Height Above Buoyancy

The fast sliding of ice streams is aided by large basal water pressures. An early suggestion is that these pressures are linked to the depth below sea level [*Budd et al.*, 1979]. The implication is that there is a free water connection between the ice sheet base and the ocean so that the effective pressure at the bed is equal to the height of the ice above ocean buoyancy. There is evidence for ponded water far in the interior at Byrd Station [*Whillans and Johnsen,* 1983] and under the ice streams [*Shabtaie et al.*, 1987; *Bentley et al.*, 1998]; such ponding implies pressures vastly in excess of that expected from the depth below sea level. In the case of UpB, the height-above-ocean-buoyancy model leads to a calculated difference between overburden and water pressures that is a factor of 50 too large [*Bentley,* 1987]. This model underestimates basal water pressure.

Possibly basal water pressure plays a role, but it cannot be the dominant parameter. For example, basal pressures are close to the glacial-overburden pressure near Byrd Station, yet motion is slow. At the other extreme, basal pressures are at buoyancy for the ice shelf where motion is fast. Something else, such as the roughness and strength of the bed must dominate the determination of basal drag.

Deforming Bed

A series of papers describes the view that a laterally continuous viscous stratum may exist between the glacier and the static bedrock beneath [*Alley et al.*, 1986, 1987; *MacAyeal,* 1994]. Based on seismic imagery, the stratum is some 0 to 13 m thick. The hypothesis is that shearing through this stratum of till accounts for much of the motion of the ice stream and is a process for horizontal transport of debris. A prediction of this model, shared with other models, is the presence of a till delta at the mouth of the ice stream. As noted above, such a till delta may have been found.

This model for control of ice stream motion seemed particularly attractive when basal drag was believed to be significant at the bed and the bed to consist continuously of soft sediment of appropriate viscosity. However, it is now known that basal drag is very small under active ice stream B, the ongoing mechanical control instead coming from the ice stream sides. Also samples recovered from the bed have large porosity and extreme weakness (2 kPa; *Kamb* [1991]). The water content of the debris is similar to that of mudflows which have viscosities (0.03×10^{-12} to 3×10^{-12} kPa-a, Table 5 in *Iverson* [1997]) many orders of magnitude weaker than that proposed for beneath ice streams (0.2 kPa-a [*Alley et al.*, 1986; *Jenson et al.*, 1996]). Most basal deformation must be plastic very near the ice-bed contact [*Kamb,* 1991] and have little direct control on ice stream motion.

In places, the ice stream could be dragging along some debris [*Tulaczyk et al.*, 1998]. Moreover, there is the possibility that this debris is collected at potential sticky spots under the ice stream, keeping the bed consistently smooth and drag resistant.

Moldable Bed

It seems probable that the bed can deform, although perhaps not continuously in either space or time [*Hindmarsh,* 1997]. In fact, considering that ice velocity and thickness change with time in at least minor ways on the ice stream, the bed of the ice stream must be continuously reformed to maintain small friction. This can happen if the bed is moldable such that sites that tend to oppose flow are removed.

This model has some of the weaknesses of other models. For example, it does not explain the abrupt change in speed at lateral margins nor why the bed under interstream ridges is strong. Maybe if erosion rate is linked with some power-law product of slippage rate and drag then there may be an accounting for these

characteristics. Also, the model does not explain why the middle and lower reaches of ice stream C stopped.

A variation in emphasis on this model (or the deforming bed model) is that a layer of sedimentary rock beneath the ice is needed for fast flow. *Bell et al.* [1998] and *Anandakrishnan et al.* [1998] use remote sensing methods to infer that there are sedimentary rocks under part of the catchment to ice stream C. Observed ice speed is somewhat faster over some of the sedimentary rock than over igneous rock and other sedimentary rock. They interpret the faster speed as being ice-stream behavior, although it does not fit the definition of ice stream used here. *Bell et al.* [1998] propose further that very thick (much more than 100 m) sedimentary rock is needed for fast flow, but the physical reason for this is not clear. Perhaps the issue is that a certain moldable type of sedimentary rock can be formed into a more streamlined bed that offers less friction.

Ongoing Surge

A suggestion is that the ice stream systems could be in various stages of surge cycles. Surges are known for certain valley glaciers and are associated with ice speed increases of 10 to 100 fold with time. Part of the upper portion of the glacier is depleted during a surge and extra ice is transported to the ablation zone. After the surge phase, the glacier nearly stops and the depleted zone is rebuilt while the surge lobe decays. Often a new surge occurs after recovery. The ice streams do have speeds that are about 100 times faster than the neighboring interstream ridge ice and mass balance measurements do indicate thinning in the catchment of ice stream B. The suggestion is that the lower and middle reaches of ice stream C are at a post-surge phase and the surge lobes of extra ice are in the ice shelf [*Casassa et al.*, 1991] where they dissipate.

By comparing early mass balance calculations along ice stream B [*Shabtaie et al.*, 1988] with the results of a numerical model *Bindschadler* [1997] suggests that ice streams are the result of a sudden weakening of ice strength and flow resistance. These calculations of mass imbalance are suspect, as explained above. Bindschadler further suggests that there is an ongoing headward migration of ice stream onsets, although the kinematic wave analysis is based on a model of basal sliding that does not accord with observations.

A convincing demonstration of surge activity would require evidence of the surge cycle. Perhaps the remnants of formerly active ice stream segments (c.f. Changes with Time, above) are surge-depleted zones that are now in a build up stage. The one such site checked (the Unicorn, ridge B1/B2) is currently thickening [*Hamilton et al.*, 1998]. Maybe the fast ice streams are in full surge stage. The growing bulge in the upper reach of ice stream C, between the active and inactive portions of ice stream C, could be called a surge front. As yet, the existence of surges in Antarctica is an unproved possibility.

Whether the ice streams surge may not be a question distinct from others addressed here. Surging is a descriptive term for cyclic thickening and thinning of glaciers; it does not describe a physical process. For a cause of the changes one must invoke some other hypothesis.

Active Volcanoes

A subglacial structure having the shape of a composite volcano has been found under the inland ice upglacier of ice stream B/ice stream C. *Blankenship et al.* [1993] propose that the surface moat or depression to the side is not the result of ice flow around the volcano, but is due to basal melting associated with volcanism. Active subglacial volcanism or focused geothermal heat flow is a possibility in this region of thinned and stretched crust. However, a link between volcanoes and ice streams in position and time of activity has not been established. In Iceland, volcanic activity and fast glacier motion are temporally independent [*Björnsson*, 1998].

Global Warming

A common public perception is that the ice sheets are sensitively vulnerable to a global warming. This view is advanced in the title and header to the review by *Oppenheimer* [1998]. The implication is that there is evidence of a tendency toward century scale dramatic change. We are not aware of any such evidence, and none is presented by Oppenheimer.

CONCLUSIONS

The first mystery of why the ice streams are so fast despite small gravitational driving stress is partly resolved. There is a switch at the onset to ice stream flow where the bed becomes extremely weak, offering almost no friction. Thereafter, ice stream motion is restrained by friction from the sides and maybe from some rough areas within the ice stream. Basically, there is a change from control at the bed to control at the sides.

Several important physical processes involved in the first mystery await resolution. For example, the reason why the bed is so weak and why it remains weak is not established. Also, the processes operating at the lateral margins are not even fully identified, let alone properly modeled. For example, *Van der Veen and Whillans* [1996] model that a widening ice stream should become faster, yet the observations show the reverse, slowing during widening. Important as the remaining issues may be, the community has efficiently sorted out the broad issue involved in the first mystery: the ice streams are fast because their bases are nearly frictionless.

The second mystery is the discovery of rapid changes in the ice sheet. An explanation for the changes is not now available, but the explanation must be associated with the process responsible for weak beds, this process must lead to instabilities. A proper resolution of this second mystery requires an understanding of what keeps the beds frictionless and what changes friction.

These mysteries have implications beyond that of the cause of ice streams and the stability of the West Ant-

arctic Ice Sheet. Their solutions will be important to deducing the physical reasons for the major fluctuations of other ice sheets, such as the Laurentide Ice Sheet and Scandinavian Ice Sheet, which also operated on soft beds and which also underwent rapid time fluctuations.

APPENDIX

Transverse Variation in Stress and Velocity

The distribution of stress and velocity across an ice stream is developed from theoretical principles. Here the theory behind the comparison with observation in Figure 6 is developed.

Balance of forces is considered for a column of unit map area. Let the coordinate x represent the along-flow axis and y across flow. Let τ_{bx} represent drag at the bed. The motive effect of gravity is described by τ_{dx}, the driving stress. Depth-averaged stresses acting on vertical faces of the column are R_{xx} (longitudinal normal) and R_{xy} (lateral drag). The stresses associated with longitudinal tension or compression and with lateral drag are large in the upper, cold portion of the glacier, and smaller at depth. In the present analysis, mean values through the thickness, H, are used. The balance of the various forces acting on the column is described by [*Van der Veen and Whillans*, 1989]:

$$\tau_{dx} = \tau_{bx} - \frac{\partial}{\partial} HR_{xx} - \frac{\partial}{\partial y} HR_{xy} \qquad \text{(A1)}$$

The stresses are represented by the letter, R, to emphasize that they are stresses that normally Resist, or oppose the motion of the glacier.

To derive a transverse profile of speed, equation (A1) is integrated with respect to distance across the ice stream from the kinematic centerline (where $y = 0$, $R_{xy} = 0$)

$$\int_0^{HR_{xy}} \mathrm{d}(HR_{xy}) = \int_0^y \left[\tau_{bx} - \tau_{dx} - \frac{\partial}{\partial x}(HR_{xx}) \right] \mathrm{d}\bar{y} \qquad \text{(A2)}$$

Now define:

$$C = -\left[\tau_{bx} - \tau_{dx} - \frac{\partial}{\partial x}(HR_{xx}) \right] \qquad \text{(A3)}$$

and assume that C is constant across the ice stream. In fact, longitudinal force gradients (per unit width), $\partial HR_{xx} / \partial x$, are everywhere negligibly small, so they do not contribute meaningfully to any transverse variations in C. Driving stress, τ_{dx}, does vary somewhat, mainly because of transverse variations in surface slope (Figure 7). The transverse variation in basal drag, τ_{bx}, is not *a priori* known. Completing the integration of Equation (A2):

$$HR_{xy} = -C\,y \qquad \text{(A4)}$$

It is this function that is drawn as a straight line in Figure 6, for τ_{bx} and $\partial HR_{xx} / \partial x$ both set to zero. The measurements follow the line reasonable well, and so support the assumption that C is nearly constant across the ice stream and that basal drag, τ_{bx}, is indeed nearly zero.

An expression for velocity is obtained by utilizing the constitutive relation [*Hooke*, 1981]

$$R_{xy} = B\left(\frac{1}{2} \frac{\partial u_x}{\partial y} \right)^{1/3} \qquad \text{(A5)}$$

for the case of simple shear, which is a good approximation for most of the width of the ice streams (Figure 6). A depth-mean value for the rate factor, B, is used.

Combining Equations (A4) and (A5) to eliminate R_{xy}, and solving for u_x:

$$\int_{U_{max}}^{u_x} \mathrm{d}u_x = -2 \int_0^y \left(\frac{Cy}{HB} \right)^3 \mathrm{d}\bar{y} \qquad \text{(A6)}$$

which leads to glacier speed varying as the 4th power with respect to distance from the kinematic centerline.

The integral of Equation (A6) is linked with ice-stream width by invoking the criterion that the along-glacier component of velocity is zero at the shear margins $u_x(y=\pm W) = 0$, in which W represents the ice-stream halfwidth. Integrating:

$$u_x = \frac{C^3 (W^4 - y^4)}{2(HB)^3} \qquad \text{(A7)}$$

This expression is a theoretical profile of the longitudinal component of velocity across the ice stream. Most measured profiles are well approximated by this.

Values of C are needed for the computations leading to Figure 2. These are computed from centerline speeds by rearranging Equation (A7):

$$C = \frac{HB}{W} \left(\frac{2U_{max}}{W} \right)^{1/3} \qquad \text{(A8)}$$

This expression is used to evaluate the role of lateral drag along the ice stream (wherever the simple relation of Equation (A3) is valid). Lateral drag in the budget of forces is

$$\frac{\partial HR_{xy}}{\partial y} = -C = -\frac{HB}{W} \left(\frac{2U_{max}}{W} \right)^{1/3} \qquad \text{(A9)}$$

This expression allows the role of lateral drag to be estimated from ice stream geometry (H,W), centerline speed, U_{max}, and the flow law for ice. It is used to compute lateral drag (2nd panel in Figure 9).

Acknowledgements. We thank Sridhar Anandakrishnan for comment and Mike Willis for comment and for figure preparation. Supported by grants from the US NSF-OPP. Byrd Polar Research Center contribution number 1171. Geophysical and Polar Research Center, University of Wisconsin-Madison, contribution 587.

REFERENCES

Alley, R. B., D. D. Blankenship, C. R. Bentley, and S. T. Rooney, Deformation of till beneath ice stream B, West Antarctica, *Nature, 322*, 57-59, 1986.

Alley, R. B., D. D. Blankenship, C. R. Bentley, and S. T. Rooney, Till beneath ice stream B. 3. Till deformation: evidence and implications, *Journ. Geophys. Res., 92*, 8921-8929, 1987.

Alley, R. B., and I. M. Whillans, Changes in the West Antarctic Ice Sheet, *Science, 254*, 959-963, 1991.

Alley, R. B., S. Anandakrishnan, C. R. Bentley, N. Lord, and S. Shabtaie, A water-piracy hypothesis for the stagnation of ice stream C, *Ann. Glaciol., 20*, 187-194, 1994.

Anandakrishnan, S., and R. B. Alley, Stagnation of ice stream C, West Antarctica by water piracy, *Geophys. Res. Ltrs., 24*, 265-268, 1997.

Anandakrishnan, S., D. D. Blankenship, R. B. Alley, and P. L. Stoffa, Influence of subglacial geology on the position of a West Antarctic ice stream from seismic observations, *Nature, 394*, 62-65, 1998.

Anandakrishnan, S., and C. R. Bentley, Micro-earthquakes beneath ice streams B and C, West Antarctica: observations and implications, *Journ. Glaciol., 39*, 455-462, 1993.

Anandakrishnan, S., R. B. Alley, R. W. Jacobel, and H. Conway, Ice Stream C slowdown is not stabilizing West Antarctic Ice Sheet, this volume.

Atre, S. R., and C. R. Bentley, Laterally varying basal conditions under ice streams B and C, West Antarctica, *Journ. Glaciol., 39*, 507-514, 1993.

Atre, S. R., and C. R. Bentley, Indication of a dilatant bed near downstream B camp, ice stream B, *Ann. Glaciol., 20*, 177-182, 1994.

Bell, R. E., D. D. Blankenship, C. A. Finn, D. L. Morse, T. A. Scambos, J. M. Brozena, and S. M. Hodge, Influence of subglacial geology on the onset of a West Antarctic ice stream from aerogeophysical observations, *Nature, 394*, 58-62, 1998.

Bentley, C. R., Antarctic ice streams: a review, *Journ. Geophys. Res., 92*, 8843-8858, 1987.

Bentley, C. R., S. Shabtaie, D. G. Schultz, and S. T. Rooney, Continuation of glaciogeophysical survey of the interior Ross embayment (GSIRE): summary of 1984-85 field work, *Antarctic Journ. U.S., XX*, 63-64, 1985.

Bentley, C. R., N. Lord, C. Liu, Radar reflections reveal a wet bed beneath stagnant Ice Stream C and a frozen bed beneath Ridge BC, West Antarctica, *Journ. Glaciol., 44*, 157-164, 1998.

Bentley, C. R., B. E. Smith, and N. E. Lord, Radar studies on Roosevelt Island and Ice Stream C, *Antarctic Journ. U.S.*, in press.

Bindschadler, R., Siple Coast Project research of Crary Ice Rise and the mouths of Ice Streams B and C, West Antarctica: review and perspectives, *Journ. Glaciol., 39*, 539-552, 1993.

Bindschadler, R., Actively surging West Antarctic ice streams and their response characteristics, *Ann. Glaciol., 24*, 409-414, 1997.

Bindschadler, R. A., S. N. Stephenson, D. R. MacAyeal, and S. Shabtaie, Ice dynamics at the mouth of ice stream B, Antarctica, *Journ. Geophys. Res., 92*, 8885-8894, 1987.

Bindschadler, R., and P. Vornberger, AVHRR imagery reveals Antarctic ice dynamics, *EOS, 71*, 741-742, 1990.

Bindschadler, R., P.L. Vornberger, and S. Shabtaie, The detailed net mass balance of the ice plain on Ice Streams B, Antarctica: a geographic information system approach, *Journ. Glaciol., 39*, 471-482, 1993.

Bindschadler, R., P. Vornberger, D. Blankenship, T. Scambos, and R. Jacobel, Surface velocity and mass balance of Ice Streams D and E, West Antarctica, *Journ. Glaciol., 42*, 461-475, 1996.

Bindschadler, R., and P. Vornberger, Changes in the West Antarctic ice sheet since 1963 from declassified satellite photography, *Science, 279*, 689-692, 1998.

Björnsson, H., Hydrological characteristics of the drainage system beneath a surging glacier, *Nature, 395*, 771-774, 1998.

Blankenship. D. D., Seismological investigations of a West Antarctic ice stream, Ph.D. thesis, University of Wisconsin-Madison, 1989.

Blankenship, D. D., C. R. Bentley, S. T. Rooney, and R. B. Alley, Seismic measurements reveal a saturated, porous layer beneath an active Antarctic ice stream, *Nature, 322*, 54-57, 1986.

Blankenship, D. D., C. R. Bentley, S. T. Rooney, and R. B. Alley, Till beneath ice stream B. 1. Properties derived from seismic travel times, *Journ. Geophys. Res., 92*, 8903-8911, 1987.

Blankenship, D. D., R. E. Bell, S. M. Hodge, J. M. Brozena, J. C. Behrendt, and C. A. Finn, Active volcanism beneath the West Antarctic ice sheet and implications for ice-sheet stability, *Nature, 361*, 526-529, 1993.

Budd, W. F., P. L. Keage, and N. A. Blundy, Empirical studies of ice sliding, *Journ. Glaciol., 23*, 157-170, 1979.

Casassa, G., K. C. Jezek, J. Turner, and I. M. Whillans, Relict flow stripes on the Ross Ice Shelf, *Ann. Glaciol., 15*, 132-138, 1991.

Clarke, T. S., and C. R. Bentley, High-resolution radar on ice stream B2, Antarctica: measurements of electromagnetic wave speed in firn and strain history from buried crevasses, *Ann. Glaciol., 20*, 153-159, 1994.

Clarke, T. S., C. Liu, N. E. Lord, and C. R. Bentley, Evidence for a recently abandoned shear margin adjacent to Ice Stream B2, Antarctica, from ice-penetrating radar measurements, *Journ. Geophys. Res.*, in press.

Drewry, D. J., *Antarctica: glaciological and geophysical folio*, Cambridge, University of Cambridge, Scott Polar Research Institute, 1983.

Echelmeyer, K. A., W. D. Harrison, C. Larson, and J. E. Mitchell, The role of the margins in the dynamics of an active ice stream, *Journ. Glaciol., 40*, 527-538, 1994.

Echelmeyer, K. A. and W. D. Harrison, Ongoing margin migration of Ice Stream B, Antarctica, *Journ. Glaciol., 45*, 361-369, 1999.

Engelhardt, H., and B. Kamb, Basal sliding of ice stream B, West Antarctica, *Journ. Glaciol., 44*, 223-230, 1998.

Engelhardt, H., N. Humphrey, B. Kamb, and M. Fahnestock, Physical conditions at the base of a fast moving Antarctic ice stream, *Science, 248*, 57-59, 1990.

Gudmundsson, G. H., C. F. Raymond, and R. Bindschadler, The origin and longevity of flow stripes on Antarctic ice streams, *Ann. Glaciol., 27*, 145-152, 1998.

Hambrey, M. J., and F. Müller, Structures and ice deformation in the White Glacier, Axel Heiberg Island, Northwest Territories, Canada, *Journ. Glaciol., 20*, 41-66, 1978.

Hamilton, G. S., I. M. Whillans, and P. J. Morgan, First point measurements of ice-sheet thickness change in Antarctica, *Ann. Glaciol., 27*, 125-129, 1998.

Harrison, W. D., K. A. Echelmeyer, and C. F. Larsen, Measurement of temperature in a margin of ice stream B, Antarctica: implications for margin migration and lateral drag, *Journ. Glaciol., 44*, 615-624, 1998.

Herzfeld, U. C., The 1993-1995 surge of Bering Glacier (Alaska) – a photographic documentation of crevasse patterns and environmental changes, *Trierer Geographische Studien, Heft 17*, 1998.

Hindmarsh, R. C. A., Deforming beds: viscous and plastic scales of deformation, *Quatern. Sci. Rev., 16*, 1039-1056, 1997.

Hodge, S. M., and S. K. Dopplehammer, Satellite images of the onset of streaming flow of ice streams C and D, West Antarctica, *Journ. Geophys. Res., 101*, 6669-6677, 1996.

Hooke, R. LeB., Flow law for polycrystalline ice in glaciers: comparison of theoretical predictions, laboratory data, and field measurements, *Rev. Geophys. Space Phys., 19*, 664-672, 1981.

Hughes, T.J., *Ice Sheets*, Oxford, U.K., Oxford University Press, 343 pp., 1998.

Hulbe, C. L., and I. M. Whillans, Evaluation of strain rates on ice stream B, Antarctica, obtained using GPS phase measurements, *Ann. Glaciol., 20*, 254-262, 1994.

Hulbe, C. L., and I. M. Whillans, Weak bands within Ice Stream B, West Antarctica, *Journ. Glaciol., 43*, 377-386, 1997.

Iverson, R. M., The physics of debris flows, *Rev. Geophys., 35*, 245-296, 1997.

Jackson, M., and B. Kamb, The marginal shear stress of ice stream B, West Antarctica, *Journ. Glaciol., 43*, 415-426, 1997.

Jacobel, R. W., A. M. Gades, D. L. Gottschling, S. M. Hodge, and D. L. Wright, Interpretation of radar-detected internal layer folding in West Antarctic ice streams, *Journ. Glaciol., 39*, 528-537, 1993.

Jacobel, R. W., and B. J. Gommes, Internal layer folding patterns from radar studies of ice streams B and C, *Antarctic Journ. U.S., 29*, 66-68, 1994.

Jacobson, H. P., and C. F. Raymond, Thermal effects on the location of ice stream margins, *Journ. Geophys. Res., 103*, 12111-12122, 1998.

Jenson, J. W., D. R. MacAyeal, P. U. Clark, C. L. Ho, and J.C. Vela, Numerical modeling of subglacial sediment deformation: implications for the behavior of the Lake Michigan Lobe, Laurentide Ice Sheet, *Journ. Geophys. Res., 101*, 8717-8728, 1996.

Jenssen, D., W. F. Budd, I. N. Smith, and U. Radok, On the surging potential of polar ice streams, Part II: ice streams and physical characteristics of the Ross Sea drainage basin, West Antarctica. Cooperative Institute for Research in Environmental Sciences, University of Colorado at Boulder, report DE/ER/60197-3, 1985.

Joughin, I., L. Gray, R. Bindschadler, S. Price, D. Morse, C. Hulbe, M. Karim, and C. Werner, Tributaries of West Antarctic ice streams by RADARSAT interferometry, *Science, 286*, 283-286, 1999.

Kamb, B., Rheological nonlinearity and flow instability in the deforming bed mechanism of ice stream motion, *Journ. Geophys. Res., 96*, 16585-16595, 1991.

Kamb, B., Basal zone of the West Antarctic ice streams and its role in their streaming motions, this volume.

Liu, C., C. R. Bentley, and N. Lord, C axes from radar depolarization experiments at UpB in 1991-92, Antarctica, *Ann. Glaciol., 20*, 169-176, 1994.

Liu, C., C. R. Bentley, and N. Lord, Velocity difference between the surface and the base of Ice Stream B, West Antarctica, from radar-fading pattern experiments, *Ann. Glaciol., 29*, in press.

MacAyeal, D. R., Large-scale ice flow over a viscous basal sediment: theory and application to ice stream B, Antarctica, *Journ. Geophys. Res., 94*, 4071-4087, 1989.

Meier, S., Portrait of an Antarctic outlet glacier, *Hydrological Sciences – Journal des Science Hydrologiques, 28*, 430-416, 1983.

Merry, C. J., and I. M. Whillans, Ice-flow features on ice stream B, Antarctica, revealed by SPOT HRV imagery, *Journ. Glaciol., 39*, 515-527, 1993.

Novick, A. N., C. R. Bentley, and N. Lord, Ice thickness, bed topography, and basal reflection coefficients from radar sounding, Upstream B, West Antarctica, *Ann. Glaciol., 20*, 148-152, 1994.

Oppenheimer, M., Global warming and the stability of the West Antarctic ice sheet, *Nature, 393*, 325-332, 1998.

Payne, A. J., Dynamics of the Siple Coast ice streams, West Antarctica: results from a thermomechanical ice sheet model, *Geophys. Res. Ltrs, 25*, 3173-3176, 1998.

Price, S. F., and I. M. Whillans, Delineation of a catchment boundary using velocity and elevation measurements, *Ann. Glaciol., 27*, 140-144, 1998.

Raymond, C. F., K. A. Echelmeyer, I. M. Whillans and C. S. M. Doake, Ice stream shear margins, this volume.

Retzlaff, R., N. Lord, and C. R. Bentley, Airborne radar studies: ice streams A, B, and C, West Antarctica, *Journ. Glaciol., 39*, 495-506, 1993.

Retzlaff, R., and C. R. Bentley, Timing of stagnation of ice stream C, West Antarctica, from short-pulse-radar studies of buried surface crevasses, *Journ. Glaciol., 39*, 553-561, 1993.

Robin, G. de Q., S. Evans, D. J. Drewry, C. H. Harrison, and D. L. Petrie, Radio-echo sounding of the Antarctic ice sheet, *Antarctic Journ. U.S., V*, 229-232, 1970.

Rooney, S. T., Subglacial geology of ice stream B, West Antarctica, Ph.D. Thesis, University of Wisconsin-Madison, 1987.

Rooney, S. T., D. D. Blankenship, R. B. Alley, and C. R. Bentley, Till beneath ice stream B. 2. Structure and continuity, *Journ Geophys. Res., 92*, 8913-8920, 1987.

Rose, K. E., Radio echo sounding studies of Marie Byrd Land, Antarctica, Ph.D. thesis, University of Cambridge, 1978.

Rose, K. E., Characteristics of ice flow in Marie Byrd Land, Antarctica, *Journ. Glaciol., 24*, 63-74, 1979.

Scambos, T. A., and R. Bindschadler, Complex ice stream flow revealed by sequential satellite imagery, *Ann. Glaciol., 17*, 177-182, 1993.

Schultz, D. G., L. A. Powell, and C. R. Bentley, A digital recording system for echo studies on ice sheets, *Ann. Glaciol., 9*, 206-210, 1987.

Sclater, J. G., C. Jaupart, and D. Galson, The heat flow through oceanic and continental crust and the heat loss of the Earth, *Rev. Geophys. Space Phys., 18*, 269-311, 1980.

Shabtaie, S., and C. R. Bentley, West Antarctic ice streams draining into the Ross Ice Shelf: configuration and mass balance, *Journ. Geophys. Res., 92*, 1311-1336, 1987.

Shabtaie, S., I. M. Whillans, and C. R. Bentley, The morphology of ice streams A, B, and C, West Antarctica, and their environs, *Journ. Geophys. Res., 92*, 8865-8883, 1987.

Shabtaie, S., and C. R. Bentley, Ice-thickness map of the West Antarctic ice streams by radar sounding, *Ann. Glaciol., 11*, 126-136, 1988.

Shabtaie, S., C. R. Bentley, R. A. Bindschadler, and D. R. MacAyeal, Mass balance studies of ice streams A, B, and C and possible surging behavior of ice stream B, *Ann. Glaciol., 11*, 137-149, 1988.

Spikes, B., B. Csatho, and I. Whillans, Airborne laser profiling of an Antarctic ice stream for change detection, *Int. Arch. Photogram. Remote Sensing, 32 (part 3-W14)*, 169-175, 2000.

Stephenson, S. N. and R. A. Bindschadler, Observed velocity fluctuations on a major Antarctic ice stream, *Nature, 334*, 695-697, 1988.

Stephenson, S. N., and R. A. Bindschadler, Is ice-stream evolution revealed by satellite imagery? *Ann. Glaciol., 14*, 273-277, 1990.

Swithinbank, C., Antarctica. U.S. Geological Survey Professional Paper 1386-B, 278 pp., 1988.

Tulaczyk, S., H. Engelhardt, B. Kamb, and R. P. Scherer, Sedimentary processes at the base of a West Antarctic ice stream, constraints from textural and compositional properties of subglacial debris, *Journ. Sedimentary Res., 68*, 487-496, 1998.

Ueda, H. T., and D. E. Garfield, Deep core drilling at Byrd Station, Antarctica, *IAHS Publ. No 86*, 53-62, 1970.

USGS, Experimental Edition maps, Antarctica Satellite Image Maps, U.S. Geological Survey, Reston VA 22092 U.S.A., 1992.

Van der Veen, C. J., and I. M. Whillans, Force budget: I. Theory and numerical methods, *Journ. Glaciol., 35*, 53-60, 1989.

Van der Veen, C. J., and I. M. Whillans, Model experiments on the evolution and stability of ice streams, *Ann. Glaciol., 23*, 129-137, 1996.

Van der Veen, C. J., Fracture mechanics approach to penetration of surface crevasses on glaciers, *Cold Regions Sci. Technol., 27*, 31-47, 1998.

Venteris, E. R., and I. M. Whillans, Variability of accumulation rate in the catchments of ice streams B, C, D and E, Antarctica, *Ann. Glaciol., 27*, 227-230, 1998.

Vornberger, P. L., and I. M. Whillans, Crevasse deformation and examples from ice stream B, Antarctica, *Journ. Glaciol., 36*, 3-9, 1990.

Whillans, I. M., Reaction of the accumulation zone portions of glaciers to climatic change, *Journ. Geophys. Res., 86*, 4274-4292, 1982.

Whillans, I. M., and R. Bindschadler, Mass balance of ice stream B, *Ann. Glaciol., 11*, 187-193, 1988.

Whillans, I. M., and S. J. Johnsen, Longitudinal variations in glacial flow: theory and test using data from the Byrd Station Strain Network, *Journ. Glaciol., 29*, 79-97, 1983.

Whillans, I. M., and K. C. Jezek, Folding in the Greenland Ice Sheet, *Journ. Geophys. Res., 92*. 485-493, 1987.

Whillans, I. M., Y. H. Chen, C. J. van der Veen, and T. J. Hughes, Force budget: III. Application to three-dimensional flow of Byrd Glacier, Antarctica, *Journ. Glaciol., 35*, 68-80, 1989.

Whillans, I. M., and C. J. van der Veen, Patterns of calculated basal drag on ice streams B and C, Antarctica, *Journ. Glaciol., 39*, 437-446, 1993.

Whillans, I. M., and C. J. van der Veen, New and improved determinations of velocity of ice streams B and C, West Antarctica, *Journ. Glaciol., 39*, 483-490, 1993.

Whillans, I. M., M. Jackson, and Y-H. Tseng, Velocity pattern in a transect across ice stream B, Antarctica, *Journ. Glaciol., 39*, 562-572, 1993.

Whillans, I. M., and Y-H. Tseng, Automatic tracking of crevasses on satellite images, *Cold Regions Sci. Technol., 23*, 201-214, 1995.

Whillans, I. M., and C. J. van der Veen, The role of lateral drag in the dynamics of ice stream B, Antarctica, *Journ. Glaciol., 43*, 231-237, 1997.

C. R. Bentley, Geophysical and Polar Research Center, University of Wisconsin, 1215 West Dayton Street, Madison, WI, 53706. (e-mail: bentley@geology.wisc.edu)

C. J. van der Veen, Byrd Polar Research Center and Department of Geography, The Ohio State University, 108 Scott Hall, 1090 Carmack Road, Columbus, OH 43210. (e-mail: vanderveen.1@osu.edu)

I. M. Whillans, Byrd Polar Research Center and Department of Geological Sciences, The Ohio State University, 108 Scott Hall, 1090 Carmack Road, Columbus, OH 43210. (e-mail: whillans+@osu.edu)